Interfacial Properties of C5Pe as an Asphaltene Model Compound

by

Jiebin Bi

A thesis submitted in partial fulfillment of the requirements for the degree of

Master of Science

in

Chemical Engineering

Department of Chemical and Materials Engineering

University of Alberta

Abstract

Water-in-oil (W/O) emulsions create many processing problems in petroleum industry. The enhanced stability of droplets and poor separation of emulsions are often associated with the interfacial accumulation of asphaltenes. The complex nature of asphaltenes has complicated the understanding of their interfacial behavior. Model compounds with well-defined structure and similar water-oil interfacial characteristics have provided an effective route to better understand interfacial behavior and the associated stability of emulsions. In this study, N-(1-hexylheptyl)-N'-(5-carbonylicpentyl) perylene-3,4,9,10-tetracarboxylic bisimide (in brief C5Pe) was used as a model compound for asphaltenes to understand the correlation between interfacial behavior and emulsion stability. It was found that the interfacial properties of C5Pe strongly depend on its concentration and water chemistry. At basic condition, C5Pe exhibited high interfacial activity due to ionization of –COOH groups. At higher C5Pe concentrations, the interfacial films exhibited high elasticity (G') and mechanical strength, corresponding well with rough and densely-packed film morphology and high emulsion stability. The C5Pe films formed on acidic aqueous phase showed high elasticity although the mechanical strength was low. Meanwhile, these films were less packed, and smoother with high compressibility, resulting in unstable W/O emulsions. Additionally, Ca^{2+} ions were found to rigidify C5Pe films by connecting C5Pe molecules of ionized –COOH groups at high pH.

Acknowledgments

I would like to thank my supervisors Dr. Zhenghe Xu and Dr. Qingxia Liu for their invaluable guidance and support throughout my graduate project. With their instructions, I really learned a lot in doing research.

I would also like to thank Dr. David Harbottle, Dr. Plamen Tchoukov and Dr. Erica Pensini for their insightful discussions and valuable suggestions which facilitated the progress of this project.

I am very thankful to Dr. Johan Sjöblom and his student Mathilde Isabelle Barriet for providing the asphaltene model compounds, improving experimental plans and explaining results.

I appreciate the help from Mr. Jim Skwarok, Ms. Jie Ru and Ms. Lisa Carreiro for their excellent assistance with my work. My appreciation also goes to the entire Oil Sands Extraction research group for their help and suggestions with my work.

Finally, I would like to thank the NSERC Industrial Research Chair in Oil Sands Engineering for financial support.

TABLE OF CONTENTS

LIST OF TABLES

LIST OF FIGURES

Chapter 1   Introduction

1.1. Overview on oil sands extraction

Canada has the third-largest oil reserves in the world, after Saudi Arabia and Venezuela. Of Canada's 173 billion barrels of oil reserves, 170 billion barrels are located in Alberta, and about 168 billion barrels are recoverable from bitumen (or oil sands).[1] Bitumen is a type of heavy crude oil, characterized by very high viscosity, high density, relatively high heavy metal concentrations, and a low hydrogen-to-carbon ratio in comparison with conventional crude oil.[2]

There are three major oil sands deposits in Alberta, which cover over 140,200 square kilometers.[3] Athabasca oil sands deposit is the largest with an estimated 1.3 trillion barrels of bitumen in place, followed by Cold Lake's 200 billion barrels of bitumen deposit; the third major deposit is the Peace River oil sands with around 130 billion barrels in place.[3]

The reference of Athabasca oil sands in history could be traced back to 1715, when Captain Swan reported that he found "Gum or pitch" in a river feeding.[4] In 1929, Dr. Karl A. Clark was issued a patent for the hot-water extraction process for separating bitumen from oil sands. This process laid the foundation for later commercial operations of Alberta's oil sands. Up to now, there are various methods to process oil sands. The methods could be essentially divided into two types, namely open pit mining and in situ extraction. For the first time in 2012, in situ oil sands production exceeded surface mined oil sands production in Alberta.[1] The dependence on in situ production will continue to increase in the future, as 80 per cent of Alberta's proven oil sands reserves are too deep underground to recover using mining methods.[1]

The general process flowsheet for bitumen extraction is shown in Figure 1.1. Oil sands are crushed first, and then water and additives are added to make slurry. The slurry is transferred to extraction plant using pipelines. During this process,

the bitumen liberated from sand grains and attached to air bubbles. In extraction plant, bitumen is recovered through flotation. The aerated bitumen is accumulated and collected as froth product at the top of separation cells, while the underflow is treated as tailings. Before the froth bitumen product is fed into upgrading process, froth treatment is conducted to remove water and solids by addition of diluents. The tailings are pumped to tailings pond, and the water separated from thickened tailings is used as recycle water in bitumen extraction plant.
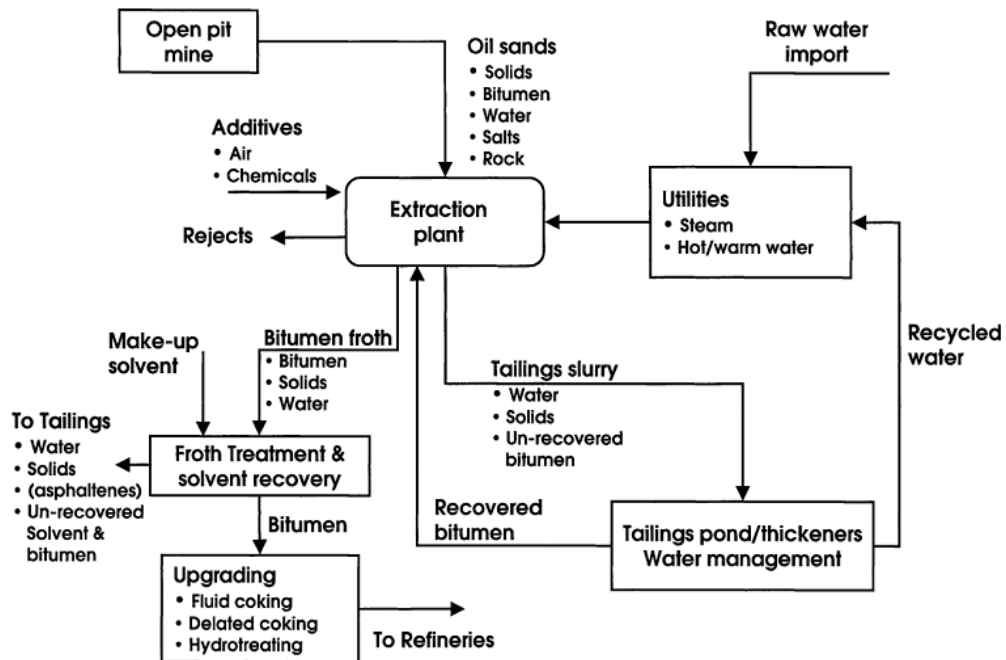
Figure 1.1 The generalized flowsheet of oil sands processing.[2]

1.2. Objectives

The objective of this thesis is to study the interfacial behavior of asphaltene model compound C5Pe and correlate emulsion stability with interfacial film properties, in an attempt to understand the stabilization mechanism of W/O emulsions. The effect of C5Pe concentration and water chemistry including pH of the aqueous phase and Ca^{2+} addition on interfacial behavior of C5Pe at water-oil interfaces will be determined.

1.3. Outline of the thesis

Chapter 1 gives a brief introduction to oil sands, including deposit areas, main production methods and generalized extraction flowsheet.

Chapter 2 reviews the literature on froth treatment technologies, petroleum emulsions and emulsion stability, and characterization of asphaltenes and asphaltene model compounds.

Chapter 3 describes the materials and setup of experimental techniques used in this study. The emulsion stability is evaluated by bottle tests. Tensionmerter, Langmuir trough, interfacial shear rheology, and crumpling ratio measurements are used to study the interfacial properties of C5Pe films. Both Brewster angle microscopy and atomic force microscopy are used to visualize the morphology of interfacial films.

Chapter 4 presents the results on the influence of C5Pe concentration on interfacial behavior of C5Pe at the water-xylene interface.

Chapter 5 studies the effect of pH and Ca^{2+} addition on interfacial properties of C5Pe.

Chapter 6 provides a general summary of this research and recommendations for future work.

Chapter 2   Literature review

2.1. Froth treatment technologies

The froth product from bitumen extraction, on average, contains 60 wt. % bitumen, 30 wt. % water and 10 wt. % solids.[2,5] The water typically contains chlorides, leading to corrosion in pipelines and upgrading equipment.[6] Solids can cause reactor beds plugging, heat exchangers fouling, and catalyst deactivation,[2] increasing the cost and complexity of operations and equipment maintenance. Therefore, the product is required to contain less than 0.5 vol. % total solids and water and have a viscosity less than 350 cSt (1 cSt = 0.01 cm^2s^{-1}).[7] The process of removing water and solids in bitumen froth is referred to as froth treatment. Since bitumen typically has a density of 1.01 g/mL[8], which is very close to that of water, the addition of a light hydrocarbon solvent (diluent) is necessary to separate water from bitumen. The diluent decreases the density of bitumen, increasing the density difference between bitumen and water. At the same time, it lowers the viscosity of bitumen. Thus the separation of water and solids is accelerated. A number of researchers have investigated the impact of diluent properties at different concentrations on froth quality. The results showed that there is a critical diluent-to-bitumen (D/B) ratio at which a number of the system properties change dramatically, see Table 2.1.[2] Depending on the diluents, the froth treatment can be classified into two types: paraffinic froth treatment (PFT) and naphtha-based froth treatment (NFT). The former process is operated at a high dilution ratio (above critical dilution) where the water-oil interface is rigid; the latter process uses low dilution ratio (below critical dilution) where the water-oil interface is flexible.

2.1.1. Paraffinic froth treatment

The onset of asphaltene precipitation was observed around critical dilution.[9] PFT process is operated at a D/B ratio above the critical dilution, where asphaltenes

are precipitated. The precipitated asphaltenes act as a carrier for undesirable impurities: emulsified water droplets and dispersed solids. Conventional settlers without rotary equipment are able to separate the aggregated impurities efficiently, and thus energy consumption is low.[2,10] Significant reduction of asphaltenes, which is the contributor to high viscosity of bitumen, greatly decreases the amount of diluent that must be blended with the bitumen in order to meet the pipelining specification for viscosity.[11] Also, the diluted bitumen product is very clean and dry, containing ~ 500 ppmw to 800 ppmw solids and ~ 100 ppmw to 300 ppmw water.[2] The very low content of water and solids makes it much easier to meet the requirements for the following upgrading and refining process. However, PFT process is operated at a higher D/B ratio than NFT process, larger equipment are needed than that required for NFT to deal with same amount of bitumen froth, increasing operating cost. In addition, the rejection of asphaltenic material to tailings leads to oil losses and recovery reduction.[10,12]
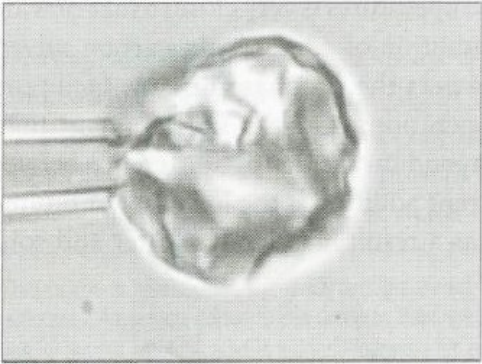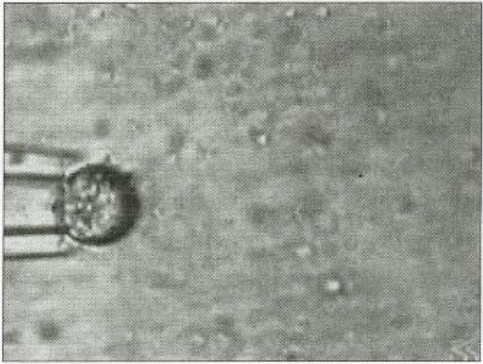
Above critical dilution Low bitumen concentration	Below critical dilution High bitumen concentration
• Rigid oil-water interface • Droplets crumple on deflation • Droplets flocculate • Paraffinic froth treatment operating regime	• Flexible oil-water interface • Droplets preserve spherical shape on deflation • Emulsions form easily • Naphtha-based froth treatment operating regime

Table 2.1 Different water-oil interfacial properties above and below critical dilution.[2]

2.1.2. Naphtha-based froth treatment

Untreated or hydrotreated naphtha is used as diluent in NFT process. The untreated naphtha is an unstable coker stream that contains slightly higher concentrations of aromatic and olefins than hydrotreated naphtha. The froth product is mixed with untreated naphtha at a D/B ratio of about 0.65 (by weight). Hydrotreated naphtha is used to satisfy new environmental restrictions that limit the type and amount of light hydrocarbon emissions. NFT process using hydrotreated naphtha requires a higher D/B ratio (~ 0.7) to achieve a comparable process performance.[12]

NFT process does not reject asphaltenes to tailings, while operating at a D/B ratio below its critical dilution. Therefore, the oil losses in NFT are much lower than in PFT. A study conducted by Shelfantook[12] compared bitumen recoveries of PFT and NFT at varying temperature and confirmed that NFT yielded higher recovery than PFT. The recovery for a two-stage mixer/settler naphtha process is around 99 % even at 80 ℃, with no dependency on operating temperature. PFT process showed a strong positive correlation between temperature and recovery. However, the recovery only achieved about 97 % at 130 ℃.[12] High recovery is a main advantage of NFT process, at the price of low quality product. The low quality of product in NFT is attributed to the fact that D/B ratio is below the critical dilution ratio. In this process, the water-oil interface is flexible and hence stable emulsions are easily formed. Long et al.[11] studied the size distribution of water droplets in naphtha diluted bitumen. They classified water into three types: (I) emulsified water, whose size is less than 10 μm in diameter, (II) dispersed water, whose size is between 10 and 60 μm, and (III) free water, whose size is larger than 60 μm.[11] Free water was found to settle very fast and extra effort is unnecessary for its removal. Sufficient time and/or additional external acceleration forces are required for settlement of dispersed water. However, the separation of emulsified water is impossible without coalescence or aggregation. NFT process needs rotary equipment such as centrifuges (with centrifugal force up to 2500 g) and

chemical aids (demulsifiers) to meet specifications for downstream operations.[2,7,11] However, the diluted bitumen product still contains ~ 1.5 wt. % to 2.5 wt. % water and ~ 0.4 wt. % to 0.8 wt. % solids.[2] The residual water is in the form of very stable water-in-diluted bitumen emulsions, and the remaining solids are fine particles that are well dispersed in the oil phase. Compared with PFT process, the operation of NFT process is more complex and operating cost is higher. Additionally, the low quality product requires the upgrading plant to use coking as the primary upgrading technology to produce synthetic crude oil, while the coke rejection-type operation is not necessary in upgrading of paraffin-diluted product.[2]

Improvement of product quality in NFT process calls for more efficient demulsifiers. To find or develop an optimal demulsifier, it is of great importance to understand the stabilization mechanism of water in diluted bitumen emulsions.

2.2. Emulsions and emulsion stability

An emulsion is a dispersive system consisting of two immiscible liquids, one is dispersed phase and the other is continuous phase.[13-15] According to Bancroft's rule, the continuous phase of an emulsion tends to be the phase in which the emulsifier is preferentially soluble. So the surfactants more soluble in water tend to form oil-in-water (O/W) emulsions, and surfactants more soluble in oil tend to form water-in-oil (W/O) emulsions.[15] The empirical expression of hydrophilic-lipophilic balance (HLB) value is widely used to describe the amphiphilic nature of surfactants.[2] Based on the equation *HLB = 7 + Σ(hydrophilic group numbers) − Σ(lipophilic group numbers)*,[16] higher HLB value indicates higher solubility in water. W/O emulsions are commonly found for HLB < 6 and O/W emulsions for HLB > 8.[16]

The most important property of an emulsion is its stability. Since large interfacial area increases total system energy, emulsions are inherently unstable. In other words, emulsion breaking should occur spontaneously to decrease the system

energy. The fact that the emulsions remain stable for weeks or months without any noticeable phase separation implies that the rate of the phase separation is extremely slow. This is called kinetic stabilization. Kinetic stabilization means that, although the system is intrinsically unstable, the phase separation is slow such that the emulsion appears to be infinitely stable.[2] This stabilization is caused by surface forces.[2] There are three main interaction forces between emulsion droplets[17]: (I) van der Waals attraction, (II) electrostatic repulsion, and (III) steric repulsion.

The van der Waals attraction between atoms or molecules stems from three types of interactions: Keesom interaction between two permanent dipoles, Debye interaction between a permanent dipole and an induced dipole, and London dispersion interaction between two transient induced dipoles. Due to the different orientations of the dipoles, the Keesom and Debye attraction forces tend to cancel. Thus, the most important is the London dispersion interaction, resulting from charge fluctuations.

There are two types of repulsions, counteracting the van der Waals attraction. One is electrostatic repulsion, which is the result of creation of electrical double layers. The adsorption of an ionic surfactant could charge the emulsion droplets. When charged droplets approach each other such that the double layer begins to overlap (i.e., the separation distance becomes less than twice the double-layer extension),[17] the repulsion occurs and prevents droplets from colliding and coalescing. The other is steric repulsion, which is the result of adsorbed non-ionic surfactants or polymer layers around emulsion droplets. Since surfactant and polymer molecules occupy a certain amount of space, their protruding parts make a close approach of emulsion droplets impossible.

The stabilization of emulsions is favorable in many commercial processes. O/W emulsions are frequently utilized in food processing, such as mayonnaise, salad creams and deserts.[17] In cosmetics, hand moisturizers, sunscreens and hair-sprays are most common emulsions, used to deliver various ingredients to hair and skin.

Moreover, nano-emulsions are applied to pharmaceuticals as adjuvants in vaccines.[18] However, the formation of stable emulsions in petroleum industry creates numerous problems. The formed emulsions can be: (I) W/O, (II) O/W and (III) multiple (W/O/W, O/W/O) emulsions,[19] and W/O emulsions are dominant and difficult to be destabilized.

Despite of years of studies, the exact stabilization mechanism of W/O emulsions has not been fully understood. However, the rigid films around water droplets have been observed by many researchers, which is of great importance to the stability of W/O emulsions.[20-22] Sjöblom et al.[23] pointed out that an emulsifying agent must be present to form stable W/O emulsions. Such agents include clay particles, added chemicals or indigenous crude oil components such as asphaltenes, resins, waxes, and naphthenic acids. It is commonly believed that asphaltenes are the main components that contribute to the stabilization of W/O emulsions.[24-31] McLean and Kilpatrick[24,25] have proposed that the W/O emulsion is stabilized by the formation of cross-linked structure of asphaltenic aggregates with mechanical strength at the water-oil interface. They also emphasized the importance of available solvating resins on emulsion stability, and the optimum emulsion was obtained at a small amount of resins (i.e. resin-to-asphaltene ratio = 0.33). The ability of inorganic solid particles to enhance the stability of W/O emulsions was also reported in literature.[19,32-35]This stabilization occurs when particles are partially wet by both phases. Fine solid particles (a few microns or less) could become interfacially active with the adsorption of resins and asphaltene aggregates from the crude oil.[35] The extent of aggregates adsorption influences the wettability of particles, and thus determines the effectiveness of solid particles in stabilization of W/O emulsions.

2.3. Asphaltenes

Asphaltenes are defined as a solubility class of material that is insoluble in straight-chain alkanes, such as pentane and heptane, but soluble in light aromatic

hydrocarbons (i.e. toluene and benzene).[2,36-38] Typically, they are separated from crude oil by precipitation upon addition of light hydrocarbon solvents as shown in Figure 2.1. SARA analysis of crude oil separates the oil into saturate, aromatic, resin, and asphaltene (SARA) fractions.[2] The saturate fraction contains non-polar linear, branched, and cyclic hydrocarbons.[2] The aromatic fraction contains molecules with one or more aromatic rings.[2] Resins and asphaltenes contain various polar groups. The polarizability of all SARA fractions increases from saturates to asphaltenes.[2] Asphaltenes are a complex mixture of different molecules with different molecular weights, compositions and polarities.[2,38] The physical and chemical properties of asphaltenes can vary, depending on the sources and how they are obtained. Asphaltenes are the most polar components of crude oil, they adsorb slowly and irreversibly at the water-diluted-bitumen interface and prevent water droplets from coalescence.[31,39] Due to the complicated nature of asphaltenes, it is difficult to study their properties and how they stabilize W/O emulsions.
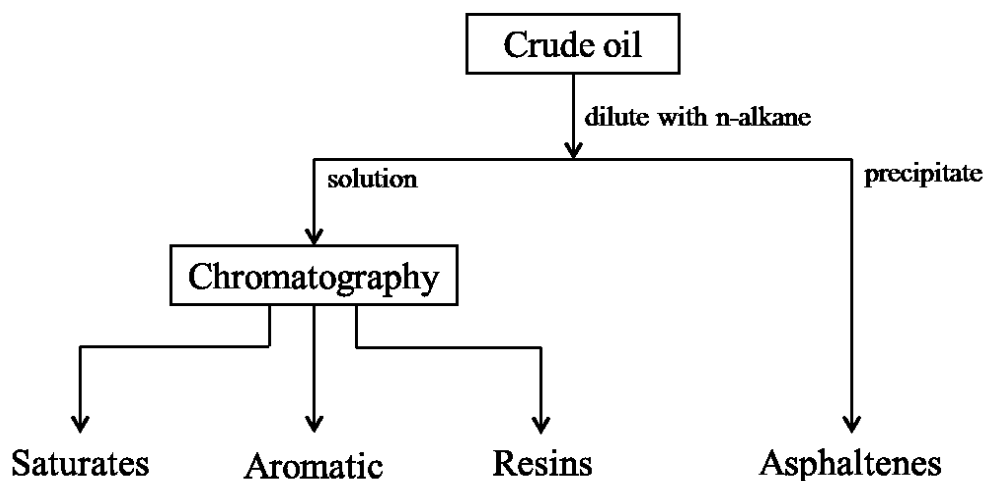
Figure 2.1 Basic scheme of characterization of crude oil fractions.

2.3.1. Elemental composition

Carbon and hydrogen are main elements in asphaltenes, accounting for around 90 % of asphaltenes in mass.[2,40-42] The atomic H/C ratio is between 1.0 and 1.2.[2,40]

10

Typically, asphaltenes contain a few percent of other atoms, called heteroatoms, such as nitrogen, oxygen and sulfur.[2] They also contain trace amounts of vanadium and nickel.[40,43] The most common techniques for determining the chemical composition of asphaltenes include combustion elemental analysis (H/C, N, S), inductively coupled plasma mass spectrometry (V, Ni, Fe), and Fourier transform infrared spectroscopy (polar functional group concentrations).[40] Some average properties of asphaltenes are showed in Table 2.2.

Table 2.2 Typical values of elemental compositions in asphaltenes.[40]

Element (wt%)	
H/C atomic	1.0–1.2
Nitrogen	1.0–1.2
Sulfur	2.0–6.0
Oxygen	0.8–2.0
Vanadium (ppm)	100–300

Chemical analysis provides valuable information to understand the molecular structure of asphaltenes. Every additional ring or double bond requires the loss of two hydrogen atoms. Thus, knowledge of the numbers of C and H atoms in a molecule determines its number of rings or equivalent double bonds.[43] Atomic H/C ratios between 1.0 and 1.2 and N, S, and O content of a few weight percent suggest that much of the asphaltene backbone consists of fused aromatic carbons interspersed with polar functional groups containing five to seven heteroatoms per molecule.[40] The specific orientation of polar and aromatic functional groups within the internal structure of asphaltene molecules is a matter of considerable controversy. FTIR analysis reveals many groups capable of forming hydrogen bonds, including carboxylic acids, carbonyls, phenols, pyrrolic, and pyridinic nitrogen.[40]

2.3.2. Molecular weight and structure

Asphaltene molecules stick together to form nanoaggregates at very low concentration, on the order of 10^{-4} mass fraction.[43] Because of asphaltene association, the debate on their molecular weight is still ongoing.

In previous studies, vapor pressure osmometry (VPO) and size exclusion chromatography (SEC), also known as gel-permeation chromatography (GPC) are primarily used for the determination of asphaltene molecular weight. VPO depends on the colligative property which is the reduction of vapor pressure due to the presence in solution of a nonvolatile component. However, VPO does not determine whether the nonvolatile component is a molecule or some type of aggregate.[44] High dilution is required to estimate the molecular weight of monomer molecule. However, the experimental errors increase significantly at high dilutions.[2] Consequently, this technique yields much larger molecular weight, in the range of 2000 Da to 10000 Da (Da = g/mol).[2,42-45] The results gained from GPC are similar to those from VPO. In GPC, molecular size is estimated based on the elution time of the investigated material from a column filled with a porous gel.[2] Large species are too big to fit into the pores of the column so they go through the column rapidly, while small species stay in the column longer.[42] This method also suffers from self-association of asphaltenes. Additionally, there is no good standard of elution time-to-molecular weight comparison for asphaltenes.[44]

Modern methods for asphaltene molecular weight measurement could be divided into two categories: mass spectrometry and molecular diffusion.[43,44] Mass spectrometry induces a charge on the molecule, accelerates the resulting ion in an electromagnetic field, and measures the charge-to-mass ratio.[43] There are various types of mass spectrometry, differing in the ways of ionizing molecules and accelerating ions, such as field-desorption/field ionization mass spectrometry (FD-FI MS), atmospheric pressure photoionization mass spectrometry (APPI MS) and field ionization mass spectrometry (FIMS). FD-FI MS results showed that asphaltenes have a molecular weight of ~ 1,000 Da with a broad distribution.[46]

APPI MS studied the molecular size of asphaltenes to be 750 Da with a range of 400 to 1200 Da.[47] FIMS gave results consistent with APPI results.[43] In molecular-diffusion measurements, various techniques, especially fluorescence techniques, track the diffusion of individual molecules. Large molecules diffuse slowly, and smaller molecules diffuse more quickly. Estimates of molecular diameter are interpreted to infer molecular weight by comparison with model compounds.[44] The first diffusion measurements of asphaltenes used time-resolved fluorescence depolarization (TRFD) to measure rotational diffusion coefficients. The results indicated that asphaltene molecular weights are ~ 750 Da, with a range of 500-1000 Da for the bulk of the population.[48] Thus, the results from TRFD diffusion measurements are in good agreements with the mass spectral results. Nuclear magnetic resonance (NMR) diffusion measurements obtain a similar but slightly larger asphaltene molecular size, resulting from some dimers or pairs of asphaltene molecules.[49] Fluorescence correlation spectroscopy (FCS) has been applied to asphaltenes by measuring translation diffusion coefficients. The FCS results reported for petroleum asphaltenes from different sources are in close accordance with results reported by TRFD.[48]

The molecular size estimation of asphaltenes plays a crucial role in understanding of their molecular structures. It is common to classify asphaltenes into continental and archipelago models according to current literature.[2,48,50-52] The continental model resembles a relatively flat disk-like molecule, with a center that has a dominant aromatic core and a periphery that is characterized by aliphatic chains. The archipelago model consists of aliphatic chains interconnecting groups of small aromatic regions.[50] Figure 2.2 shows two types of asphaltene structures, continental and archipelago model, respectively.

2.3.3. Precipitation and deposition

Asphaltenes precipitation and deposition have been reported in many situations of importance in oil production operations.[43,53,54] Deposited asphaltenes on tubules

and flow pipelines pose challenges to petroleum operations, increasing the cost of management and operation significantly. Asphaltenes deposition also leads to pronounced reduction of oil production. Understanding the mechanisms of precipitation and deposition is the first step toward solving these problems.
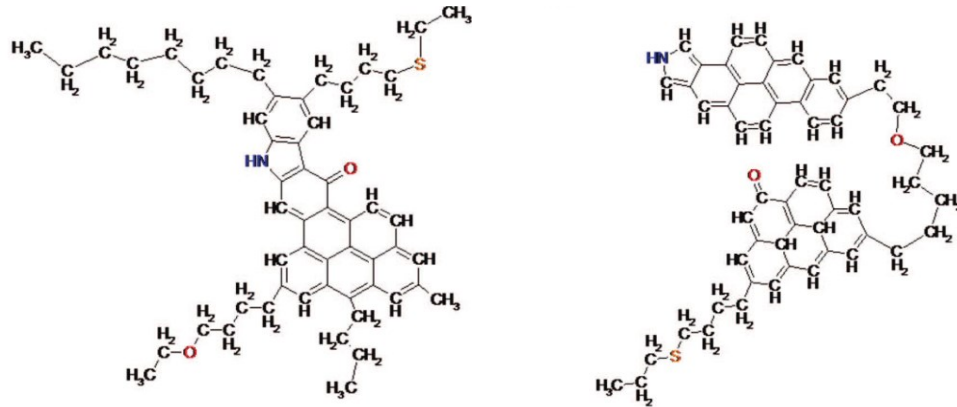
Figure 2.2 Hypothetical structures of asphaltene molecules. Left: continental model; right: archipelago model.[48]

It is well known that asphaltenes remain in thermodynamic equilibrium into solution by colloidal or solution state under reservoir conditions. The asphaltene equilibrium can be disrupted due to pressure reductions, change in temperature, change in crude oil chemical composition, and addition of miscible gases and liquids to the oil as applied in various enhanced oil recovery techniques.[55] The effect of composition and pressure on asphaltene precipitation is believed to be stronger than the effect of temperature.[56,57] Asphaltene precipitation envelope (APE) is used to describe asphaltenes precipitation phenomenon. The APE delimits the stability zones for asphaltenes in solution, see Figure 2.3.[43] During reservoir production, primary depletion causes pressure to decrease. When pressure reaches the upper APE, also known as the asphaltene-precipitation onset pressure, the least-soluble asphaltenes will be precipitated. As pressure continues to decrease, more asphaltenes will precipitate, and maximum amount of precipitation is reached at the bubble-point pressure. With continued pressure decrease, solution gas is removed from the oil. The previously precipitated

asphaltenes may begin to redissolve at the lower APE.[43,58] Numerous studies were conducted to develop asphaltenes precipitation models, for a better prediction of the location and extent of asphaltenes precipitation.[58-63] The models can be classified into two categories according to different conceptual descriptions of asphaltene solutions: (1) asphaltenes and resins are considered as molecular entities dissolved in crude oil; and (2) asphaltene and resin molecules form asphaltene–asphaltene and asphaltene–resin aggregates dispersed in an oil matrix.[58] In the first category, molecular solubility theory,[59] cubic equations of state (EOS) method[60] and statistical association fluid theory (SAFT)[61] are used to calculate the thermodynamic properties of asphaltenes. The basic assumption in second category is that a crude oil can be represented by three components: asphaltenes, resins and the solvent.[58] Thermodynamic colloidal models and thermodynamic micellization models are typical examples of second category. In the thermodynamic colloidal models, asphaltene precipitation is modeled by solving for the equilibrium between the resins absorbed in asphaltenes and the resins that are present in the solvent. Micellization models used liquid-liquid equilibrium.[62] The precipitated heavy phase is assumed to be in liquid state and to consist of only asphaltenes and resins, while light liquid phase is considered to comprise monomers of all the components and micelles.[63]
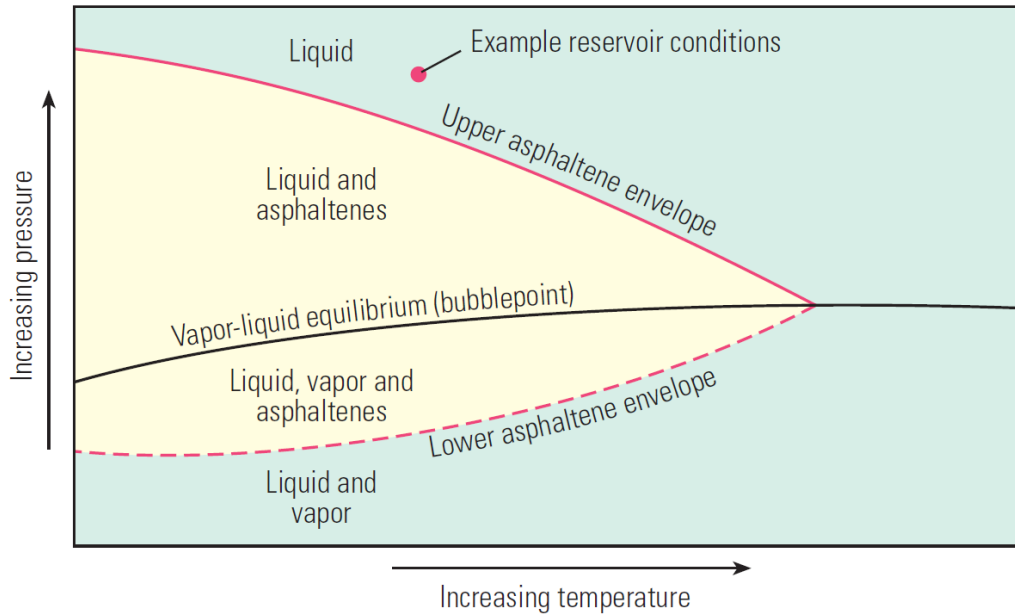
Figure 2.3 The asphaltene precipitation envelope in pressure-temperature space.[41]

Although precipitation is necessary for asphaltene deposition to take place, deposition is not a foregone conclusion.[64] Compared with asphaltene precipitation, deposition is a much more complicated process. Additional parameters such as flow shear rate, surface type and characteristics, particle size and particle-to-surface interactions influence deposition.[43,64] Thus, it is essential to conduct deposition measurements at realistic production conditions of these parameters. The deposition tests help determine specifications and estimate the tendency and rate of deposition. Recently, Akbarzadeh and his coworkers[64] transformed the previous high-pressure closed-chamber design into a dynamic one, and the samples containing low asphaltene concentrations were successfully tested. The lower deposition rate was found at higher Reynolds number of the fluid and higher shear stress on the deposit.

2.3.4. Interfacial properties

Previous work on asphaltenes demonstrated the formation of rigid or "skin-like" layers at water-oil interfaces,[65,66] which related to the significant increase in

stability of W/O emulsions due to the increased stability of asphaltene-stabilized films surrounding water droplets.[67] To understand the properties of asphaltene-stabilized films, researchers and engineers applied various techniques to study their behavior at interfaces, such as interfacial tension, crumpling ratio, Langmuir trough, and rheological measurements.

Crumpling ratio ($CR = \frac{A_f}{A_i}$, where A_f is the projected area of droplet when crumpling was first observed, A_i is the initial projected area of droplet.) measurements provide a way to quantitatively evaluate the degree of skin formation.[68-70] Larger crumpling ratio indicates the formation of more rigid skins. By applying micromechanical volume contraction experiments, Gao et al.[69] measured the crumpling ratios of bitumen components. The results gained from bitumen, asphaltenes, and maltenes are shown in Figure 2.4. For both bitumen and asphaltenes, crumpling was not observed at very low concentrations. At higher concentrations, crumpling ratio of asphaltenes increased monotonically with concentration. While bitumen showed a reduction in crumpling ratio after a sharp increase around 10^{-3} wt. %, which was attributed to the competitive adsorption of asphaltenes and maltenes in bitumen. For maltenes, no crumpling was observed at any concentration. They concluded that the irreversible adsorption of asphaltenes leads to rigidity of emulsified water droplets. In addition, sodium naphthenates (NaN) were found to soften rigid asphaltene films.[69,70]
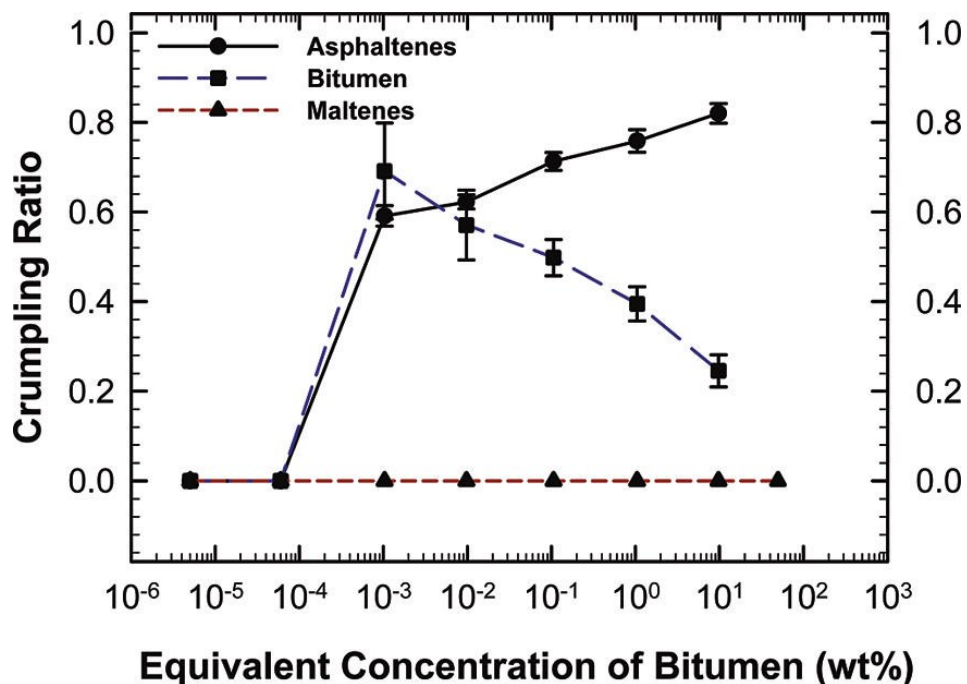
Figure 2.4 Comparison of crumpling ratio at equivalent concentration of bitumen or its components: asphaltene system (solid circle), bitumen system (solid square), and maltene system (solid triangle). The results suggest that the formation of skin at the emulsified water droplet surfaces is mainly attributed to the presence of asphaltenes.[68]

Langmuir trough experiments were conducted to characterize asphaltenes monolayer at water-air and water-oil interfaces. Ese et al.[71] studied asphaltenes extracted from crude oils of France, Venezuela and the North Sea at water-air interfaces. Different solvents were used to elucidate the ability of the solvents to prevent aggregation of the heavy fractions. The results indicated that the size of asphaltene aggregates increased when the spreading solvent becomes more aliphatic, and with increased bulk concentration. The concentration effect is more pronounced in the aliphatic than in the aromatic solvent. Later studies with asphaltenes extracted from Athabasca bitumen[72] also showed that the aromaticity of the solvent is a prime factor in the formation of aggregates and hence the rigidity of asphaltene monolayers. With increasing heptane content in heptol (the mixture of heptane and toluene), more solid asphaltene aggregates precipitated

18

and settled to the water-heptol interfaces, increasing the mass of adsorbed material. Also, the highest attainable interfacial pressure increased, exhibiting an enhanced mechanical strength. Various fractions of asphaltenes were found to behave differently at water-air and water-oil interfaces.[70,73] A monolayer of the low molecular weight asphaltene is the most expanded, while a monolayer of the high molecular weight asphaltene is the most condensed.[72] In terms of relaxation characteristics, a monolayer of the high molecular weight asphaltene relaxes most quickly. Zhang et al.[74] subsequently studied the effect of replacing the initial toluene top phase with a fresh toluene top phase on the interfacial behavior of an asphaltene monolayer at the water-toluene interface. They found that the pressure-area isotherm obtained after several washings was almost identical to that from the original asphaltene monolayer at the interface. A conclusion was drawn that asphaltene molecules in the monolayer are irreversibly adsorbed at the water-oil interface, and do not migrate from the interface to the water sub-phase or the toluene top-phase. The presence of a stable monolayer film at the water-oil interface was further confirmed in recent studies. It was reported[75] that an asphaltene monolayer is present at the water-toluene interface even though a multilayer film is initially prepared at the water-air interface first by placing an excess amount of asphaltene on a water surface. Additionally, the presence of resins or demulsifiers affects the properties of asphaltene films by rendering the films more compressible at both water-air and water-oil interfaces.[76,77]

The interfacial rheological properties of asphaltenes have been studied under two modes of deformations. The first one is dilatational deformation, referring to changing the surface area at constant shape. The second one is shear deformation, referring to changing the shape of the interface at constant area. Dilatational rheology experiments show that the interfacial asphaltene films are dominated by elasticity, which is consistent with the gradual formation of a cross-linked network on the interface.[78-80] The rheological properties were related to emulsion stability in terms of asphaltene concentration and aging time. According to tests under a wide range of asphaltene concentrations, the elastic modulus reached its

maximum value at intermediate concentration.[80] With increasing aging time, elastic modulus was found to increase at all asphaltene concentrations, while no rise in viscous modulus was observed.[80] Dilatational rheology measurements were also used to investigate the relaxation mechanisms of asphaltenes adsorbed at the water-oil interface.[81] This study indicated that the majority of asphaltenes are irreversibly adsorbed, and the reversibly adsorbed species disrupt asphaltene aggregation and weaken the network structure. The shear rheological responses of ashpaltene films were commonly determined with a biconical bob geometry.[66,82-84] Acevedo et al.[82] studied Cerro Negro crude oil and asphaltenes diluted in xylene at various pHs between 1.6 and 9.5. They claimed that the high interfacial elasticity was consistent with the high stability of these emulsions. Spiecker and Kilpatrick[66] probed the mechanical properties of asphaltenic films formed at water-oil interfaces. They observed that asphaltenes with higher concentrations of heavy metals, lower aromaticity, and higher polarity formed films of high elasticity, yield stress, and consolidation. With increasing aging time up to several hours, elasticity and yield stress of the films increased and did not appear to reach equilibrium. Due to higher degree of solvent dispersion forces, asphaltenes adsorption in solvents of greater aromaticity was slowed down and film masses reduced. Also applying the bicone technique, Fan and his co-workers investigated model oil system composed of asphaltenes and toluene-heptane mixture.[83] They claimed that the threshold concentrations are close to each other for the formation of cross-linked structure and stable W/O emulsion. The factors controlling the formation of stable emulsion are in good agreement with the interfacial elasticity of the interfacial film. In another study using two different asphaltenes extracted from crude oil and bitumen, interfacial shear rheology revealed an apparent salt-induced retardation of film growth.[84] The delayed film reorganization also depends on aqueous pH, resulting from intralayer repulsive and attractive electrostatic interactions. Utilizing a rheometer equipped with double wall ring (DWR) geometry and integrated thin film drainage apparatus, Harbottle et al.[67] recently established a direct correlation between interfacial rheological properties

of asphaltenes and droplet stability. Rapid drop coalescence (in seconds) was observed when the film microstructure is dominated by the viscous component. No coalescence occurred when the interfacial microstructure transitions to a solid-like state and the elastic contribution dominates. The authors attributed the droplet stability against coalescence to high shear yield stress and elastic stiffness of the asphaltene film.

2.4. Asphaltene model compounds

Considering the complex nature of asphaltenes, it is difficult to study the properties of asphaltenes and to understand their role in stabilization of W/O emulsions. There are two methods to solve this problem.[85] One is to fractionate the whole asphaltenes into numerous sub-fractions, determining which sub-fraction is responsible for emulsion stabilization. Different procedures have been used: multiple precipitations of asphaltenes with different n-alkane/crude oil volume ratio or toluene/n-heptane volume ratio, ultracentrifugation, and ultrafiltration.[85] However, the asphaltene fractions obtained are still very complex and polydisperse. The other method is to develop and study model compounds with well-defined structure and similar properties to real asphaltenes. Since 2005, different model compounds were proposed to mimic asphaltenes in terms of self-aggregation,[86-90] interfacial properties,[91-98] and thermal cracking[99,100].

2.4.1. Self-aggregation of model compounds

Using VPO and small-angle neutron scattering, Akbarzadeh et al.[86] studied the association behavior of pyrene based compounds in *o*-dichlorobenzene and toluene, respectively. Pyrene and alkyl-bridged dipyrene gave little association in dilute solution. In contrast, polar compounds all showed evidence for dimer formation in solution, but not more extensive association. The results suggested that polar functional groups contribute to association behavior. Later, larger alkyl polynuclear aromatic hydrocarbons were designed and synthesized to enhance the extent of self-association. The study of alkyl hexabenzocoronene (HBC)

derivatives showed that C_6-HBC tends to self-associate at temperatures up to 400 °C, unlike simple pyrene derivatives.[87] Computational studies indicated the self-association of C_6-HBC results from the interplay of alkyl-alkyl and π-π stacking interactions.[87] A bipyridyl derivative, 4,4′-bis-(2-pyren-1-yl-ethyl)-[2,2′]bipyridinyl (PBP) was used as a minimalist archipelago model of asphaltenes, and its associative properties was investigated.[88] It was found that the onset of aggregation for PBP in solution was in the same concentration range of asphaltenes with an average molecular weight of 500 – 700 Da. PBP self-associates in $CHCl_3$ and forms dimers in toluene. The authors attributed self-association of PBP to π-π interactions, with participation of both the pyrene and the pyridine groups. However, the extent of aggregation for PBP was smaller than asphaltenes in solution.

Molecular dynamics (MD) simulations were also used to study the aggregation of model molecules both in bulk and at interfaces.[50,89,90] A study by Kuznicki et al.[50] developed three different model molecules with similar molecular weights: continental model, archipelago model and anionic continental model. Analysis of the aggregate structures in single pure solvents (water, toluene, and heptane) implied that the stacking of the polyaromatic rings is the dominant structural feature of the aggregates. In binary mixtures of water and toluene, uncharged molecules did not congregate at the water-toluene interface, whereas charged terminal groups showed a distinct affinity for the water-toluene interface. Moreover, In the presence of charged entities, the resulting aggregate had a complex three-dimensional structure containing stacked polyaromatic rings. To elucidate the aggregation and partitioning of model asphaltenes in water-toluene system, Kuznicki et al.[89] conducted another study using MD simulations. In this study, two uncharged models and two charged models containing a carboxylic group were used. All model asphaltenes showed to partition completely into the toluene phase of the phase-separated solvent mixture. The positions of aggregates depended on the presence or absence of charge on these asphaltene models. The models containing charged terminal groups (COO^-) remained tethered to the

water-toluene interface, and they seemed to form hydrogen bonds with water molecules at the water-toluene interface. While uncharged models aggregated within the central region of the toluene layer, showing no interfacial activity. Furthermore, the effect of aliphatic side-chain length on the aggregation behavior of a model asphaltene in water was investigated.[90] The authors found that the extent of aggregation has a nonmonotonic relationship with the side-chain length. Asphaltene molecules with very short or very long side chains can form dense aggregates, whereas those with intermediate chain lengths cannot. Short chains have minimal interference with the π-π interactions between polyaromatic cores, whereas long side chains promote aggregation through increased θ-θ and π-θ interactions that can compensate for the reduction in the π-π interactions caused by the long side chains.

2.4.2. Interfacial properties of model compounds

Understanding the interfacial behavior of asphaltenes does ease the way to figure out the stabilization mechanism of unfavorable W/O emulsions. To elucidate how the molecular structure determines their interfacial properties and emulsion stability, Sjöblom and his colleagues[91,92,96] synthesized a series of asphaltene model molecules (Figure 2.5), utilizing an alkylated perylene core.

The solubility properties and precipitation onset of PAP and TP were studied,[91] and their precipitation showed a strong dependence on polar interactions and hydrogen bonds. Upon addition of mixture of n-heptane and toluene, the precipitation onset was around 20 vol. % n-heptane for TP and 27 vol. % for PAP. The precipitation behavior of these two model compounds fell well into the definition of real asphaltenes. The interfacial behavior was characterized by measuring the interfacial tension at the water-toluene interface (Figure 2.6).[92] All acidic compounds showed the same high interfacial activity, whereas the nonacidic BisA did not show high interfacial activity. Ionization of the carboxylic groups at pH 9 largely increased their affinity to the interface, resulting in a

higher interfacial activity. Thus the presence of acidic groups is crucial for their interfacial activity.
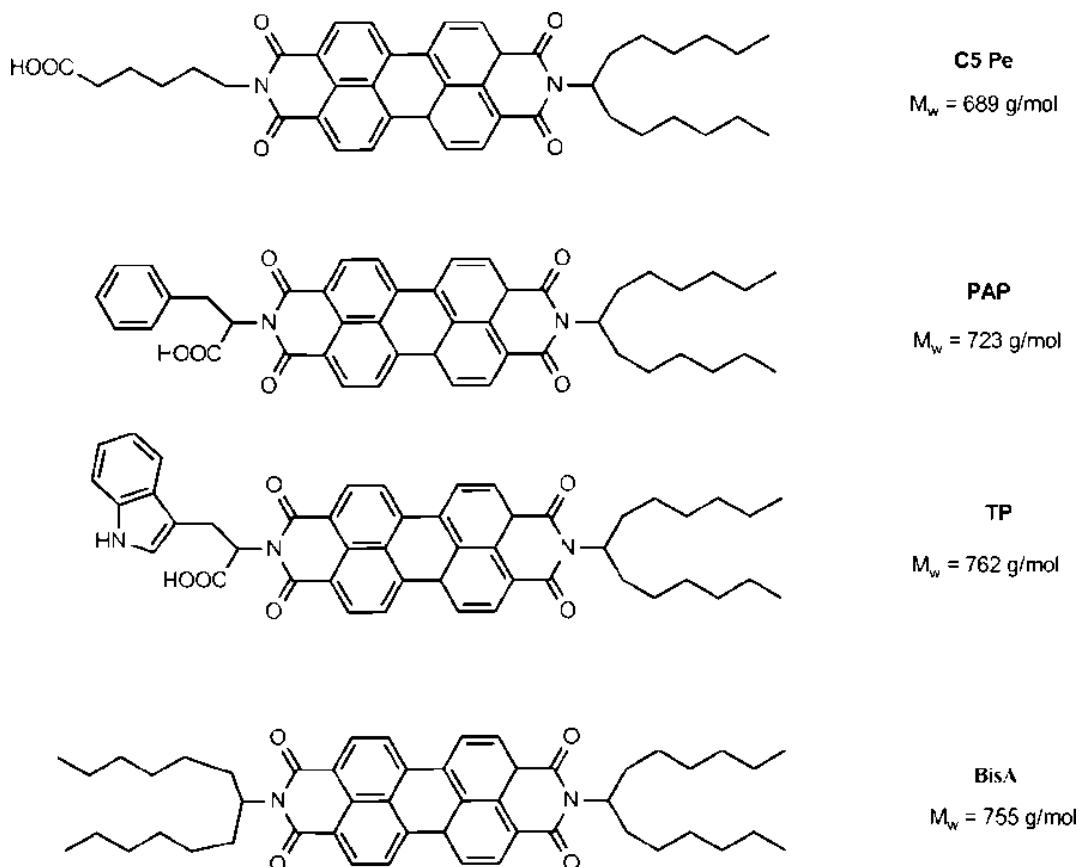
Figure 2.5 Structures, abbreviations, and molecular weights of proposed asphaltene model compounds.[92]

The study by Nordgård et al. also investigated the interfacial arrangement of asphaltene model compounds, which are shown in Figure 2.7.[92] The results indicated that acidic model compounds have a head-on geometry at interfaces with a close face-to-face stacking of aromatic cores. This efficient packing is responsible for the high interfacial activity of such compounds. Additionally, BisA possibly has a flat-on arrangement at interface since its polar groups are in the core. This study demonstrated the importance of acidic functional groups on interfacial activity and arrangement of model compounds.
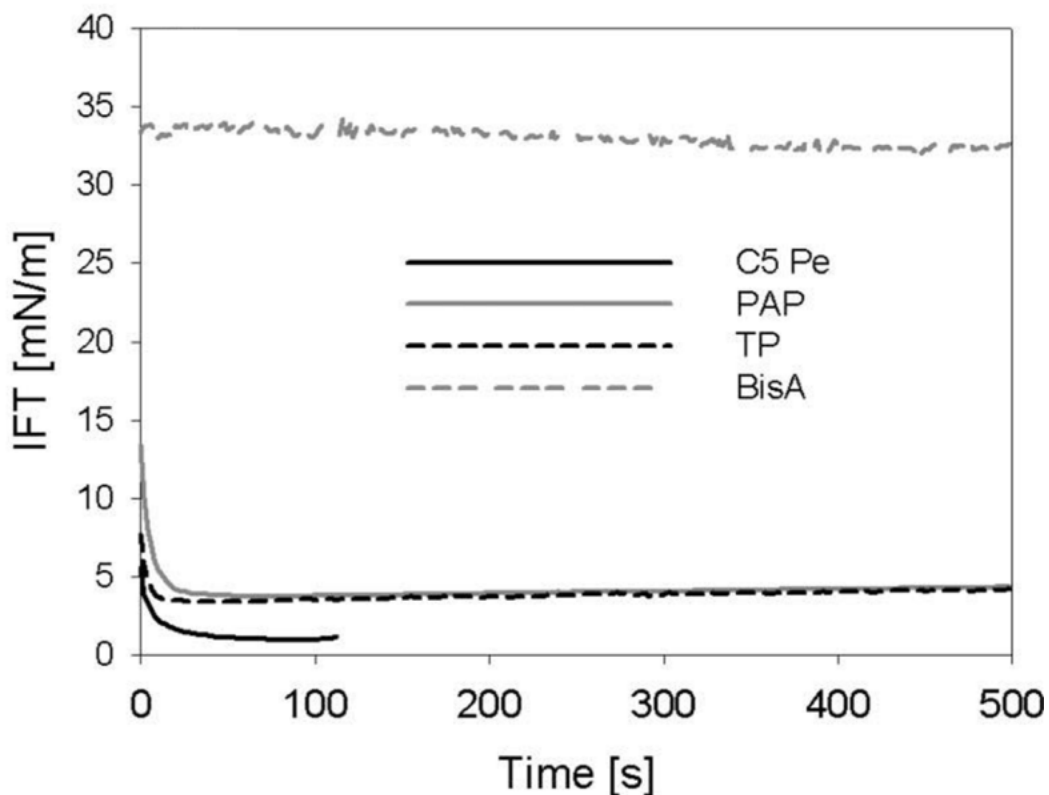
Figure 2.6 Time-dependent interfacial tension (between toluene and buffer solution of pH 9) curves at 50 μM for all model compounds.[92]

Wang et al. studied the molecular interaction of model compound C5Pe in organic solvents[93] and aqueous solutions[94] with a surface forces apparatus (SFA). They found that asphaltenes and C5Pe behave similarly in terms of adsorption behavior on model clay (mica) and molecular forces in organic solvents, such as toluene and heptane. Based on interactions of two mica surfaces across C5Pe solutions, the authors proposed a core-brush configuration of C5Pe molecules. For the interactions of C5Pe films, no significant adhesion was detected in good solvent toluene, while strong adhesion was measured in heptane. In the study of C5Pe films in aqueous solutions, water chemistry (pH, Ca^{2+}, and salt concentration) showed a strong impact on their molecular interactions. The repulsion observed between the two adsorbed C5Pe molecular layers was shown to have a steric and

electrostatic origin (due to ionization of −COOH groups). Adhesion between two C5Pe surfaces decreased sharply with increasing solution pH and salt concentration, resulting from reduction in surface hydrophobicity and hence hydrophobic attraction. Addition of Ca^{2+} ions induced the formation of large C5Pe aggregates due to strong bonding of Ca^{2+} with −COOH groups, leading to a longer range steric repulsion.
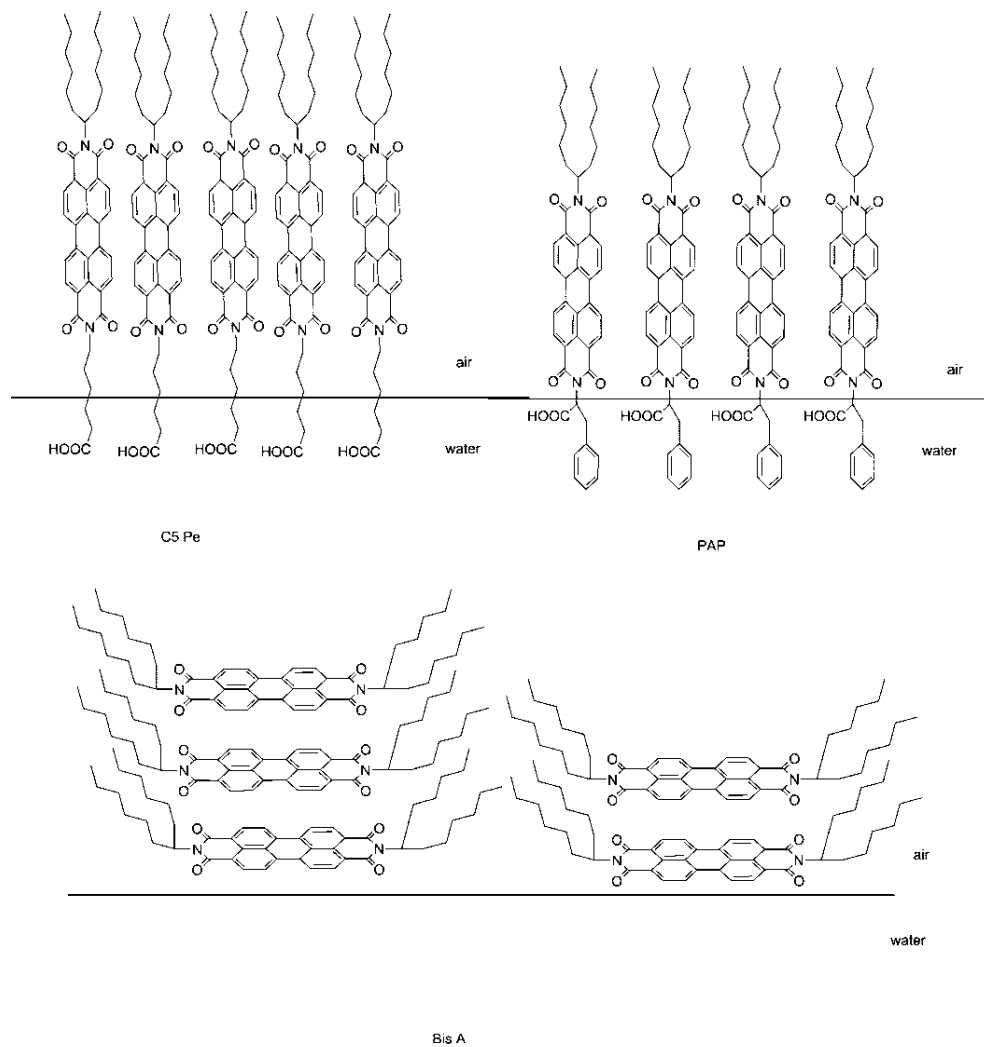
Figure 2.7 The arrangement of C5Pe, PAP, and BisA at the aqueous surface in low-compressible phases.[92]

Later, the initial partitioning of several uncharged model compounds at water-oil interface[95] was further studied using MD. Teklebrhan et al. reported the

importance of terminal moiety structure of model compounds and aromaticity of the organic phase. At the water-oil interface, the presence of hydrophobic aromatic moieties hindered the adsorption process, whereas the presence of a terminal carboxylic functional group enhanced the adsorption. Model compounds prefer to approach interface with less aromatic oil phase. C5Pe and PAP were found to preferentially adsorb at the interface in a head-on or side-on orientation with the polyaromatic core staying in the nonaqueous phase. The suggested interfacial orientation agrees well with former Langmuir trough experiment results[92].

To elucidate the relationship between molecular structure and emulsion stability, studies on the emulsification behavior of different perylene-based compounds were conducted.[96-98] Nordgård et al.[96] observed that the nonacidic compound does not form stable emulsions, while acidic compounds C5Pe and PAP give stable emulsions. Moreover, PAP was shown to stabilize emulsions to a less extent than C5Pe. NMR result and adsorption analysis for C5Pe suggested a tilted geometry of the aromatic core with respect to the interface. The bigger head group in PAP might disrupt the tilted geometry. The packing density is lower and thus the emulsion is less stable. They concluded that acidic fractions (or similar) are vital to the stability of W/O emulsions. In the study using model emulsions prepared with C5Pe in xylene and buffer of pH 8, the effect of dynamic surfactant mass transport in the dense packed layer in relation to surfactant phase partitioning after coalescence was demonstrated.[97] The results indicate that coalescence at interface could increase the concentration of surfactant in the vicinity of this interface, leading to a dynamically stabilized emulsion at this interface. That's why some initially unstable emulsions tend to be stabilized without complete separation even after very long periods of time. In another study, the mechanism and ability to stabilize W/O emulsions were compared for real asphaltenes and model compound C5Pe.[98] C5Pe was a good emulsion stabilizer at high pH, because of dissociation of the carboxylic acid groups and hence enhanced interfacial activity of the molecule. In contrast, the asphaltenes could stabilize emulsions at both

higher and lower pH values. The results showed that C5Pe describes the behaviour of asphaltenes relatively well at high pH, suggesting that only a subfraction of the asphaltenes is responsible for emulsion stabilization.

Chapter 3   Materials and experimental methods

3.1. Materials

3.1.1. Asphaltene model compound

N-(1-hexylheptyl)-N'-(5-carbonylicpentyl)perylene-3,4,9,10-tetracarboxylic
bisimide, in brief C5Pe, was used in this study to mimic asphaltenes. The protocol
utilized to synthesize C5Pe is described in previously published literature[91]. The
molecular weight of the compound is approximately 689 Da. The perylene
bisimide core of C5Pe consists of four aromatic rings, mimicking the
polyaromatic nature of asphaltenes. An aliphatic chain with a terminal carboxylic
group is attached to the core as a hydrophilic part, and a branched alkyl chain is
connected to the other side of the core as a hydrophobic part. As C5Pe has an
acidic head group, the pH determines the degree of ionization. In this study, the
experiments were conducted at pH 4, 7 or 9. Considering pKa of C5Pe at
approximately pH 6[94], the compound is fully ionized at pH 9 while the ionization
is negligible at pH 4.

3.1.2. Solvents, water chemistry and solution preparation

Xylene was used as organic solvent in this study. Xylene ($\geq$ 98.5%, ACS grade,
Fisher Scientific, Canada) comprising a mixture of ortho-, meta-, and para-
isomers was used as received. C5Pe solutions in xylene were prepared by
dissolving C5Pe in xylene and sonicated for 20 min.

The water used throughout the study was purified with a Millipore system and
had a resistivity of 18.2 mΩ/m (Milli-Q water). The pH of the water was adjusted
to required pH using buffer solutions: pH 4 (0.1 M CH_3COONa adjusted with 0.1
M CH_3COOH), pH 7 (0.1 M KH_2PO_4 adjusted with 0.1 M NaOH), and pH 9

(0.01 M Borax adjusted with 0.1 M HCl). Buffers were purchased from Fisher Scientific, Canada, and NaOH and HCl were supplied by Sigma-Aldrich.

3.2. Experimental methods

3.2.1. Emulsion preparation and bottle tests

The emulsions were prepared with a water cut of 20 % (i.e., 20:80 water-to-oil ratios by volume) by mixing 16 mL of C5Pe in xylene solution and 4 mL aqueous buffer solution. The emulsion was mixed with a homogenizer (PowerGen 1000, 125 W) at a speed of 23,000 rpm and room temperature (23 °C) for 2 min. The pH of the aqueous phase was adjusted using buffer solutions of pH 4, 7 or 9. After the homogenization, the mixture was transferred into a test glass tube sealed with a rubber-lined cap. The height of separated free water was recorded in time to evaluate the stability of emulsions. The emulsion type was confirmed by extracting a small amount of emulsion and adding it into oil or water, in order to assess which phase was the continuous phase.

3.2.2. Interfacial tension

The pendant drop method was used to measure the dynamic interfacial tension of water droplet in C5Pe in xylene solution, using a tensiometer (Theta-Lite, BiolinScientific, Sweden). Images were recorded and processed at 6 frames per second. This method involves the determination of the profile of one liquid drop suspended in another liquid.[101] The profile of the drop is determined by the balance between gravity and surface forces.[101]

In this technique, an aqueous drop was produced at the bottom of a syringe needle with the diameter of 0.84 mm in a quartz cuvette filled with C5Pe in xylene solution (~ 3 mL). Before each experiment, the syringe was thoroughly rinsed with Milli-Q water. The cuvette was washed with xylene followed by acetone. All the measurements were conducted at room temperature (~ 23 ℃). To get

equilibrium interfacial tension, all the data points were taken when the curves of dynamic interfacial tension curve plateaued (after ~ 125 min for concentrations below 0.06 mM).

3.2.3. Interfacial shear rheology

The viscoelastic properties of C5Pe at the water-xylene interface were determined using an AR-G2 stress-controlled rheometer (TA Instruments, Canada), equipped with a double-wall ring (DWR) geometry[102]. A schematic diagram is given in Figure 3.1. The DWR is made of Pt/Ir, with a radius of 35 mm. The cross section of the ring is square-edged to pin the liquid interface. To remove all the organic contaminants, the ring was flamed before each experiment. A Delrin trough with circular channel, used as the sample holder, was attached to a Peliter plate for temperature control. The temperature was kept constant at 23 ± 0.1 ℃. 19.2 mL of the aqueous solution was used as the bottom phase. Once the aqueous solution was pipetted in the cup, the ring was manually positioned at the interface and 15 mL of C5Pe in xylene solution was slowly pipetted on top of the aqueous phase. Finally, a Teflon cap was placed over the trough to prevent solvent evaporation. To study the effect of aging on C5Pe-stabilized films, time sweeps were conducted at an angular frequency of 0.5 Hz and 0.8 % strain amplitude for 100 min or 360 min. After conducting the time sweeps, frequency sweeps were performed in the range of 0.01 to 1 Hz with constant strain amplitude of 0.8 %. To determine the linear viscoelastic region, strain amplitude sweeps were conducted at the end of each experiment. During these sweeps, the angular frequency was fixed at 0.5 Hz and the strain amplitude was varied from 0.01 to 100 %.
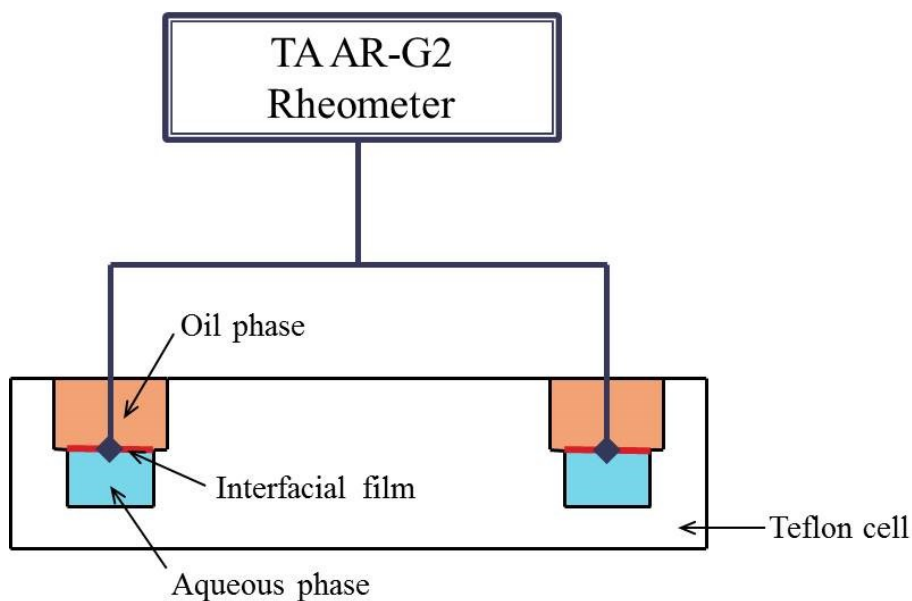
Figure 3.1 The schematic diagram of interfacial shear rheometer setup.

3.2.4. Langmuir trough experiments

The compressional behavior of C5Pe interfacial films at the water-xylene interface was probed through interfacial pressure-area isotherm measurements using a Langmuir trough. The Langmuir trough experiments were conducted using a computer controlled KSV trough (KSV Instruments, Finland) with a trough area of 170 cm^2, which is shown in Figure 3.2. A set of movable barriers is used to compress the interfacial layer by reduction of the available interfacial area. The holes in the barriers allow the top phase to flow freely without disturbing the interfacial layer. The interfacial pressure was measured using a strip of filter paper as Wilhelmy plate purchased from KSV NIMA (product id. KN 0005, Biolin Scientific). The Wilhelmy plate suspended from the electronic balance was partially immersed in the sub-phase. In the presence of interfacially active species, the interfacial pressure (π) represents the change in interfacial tension (σ) relative to the interfacial tensions of the clean interface (σ_0) and is given by:

$$\pi = \sigma_0 - \sigma \qquad (3.1)$$

Prior to each measurement, the trough was thoroughly cleaned with xylene, acetone and Milli-Q water. The lower part of the trough was filled with 120 mL of Milli-Q water buffered to the desired pH. The trough was considered clean when the pressure sensor reading was below 0.1 mN/m, with the water phase being compressed to an area of 12.5 cm^2. After setting the interfacial pressure to zero, C5Pe in xylene solution with concentrations of 0.005 mM, 0.06 mM and 0.2 mM was carefully added as top-phase, with the barriers fully open. After equilibrating the system for 30 min, the compression of the interfacial film was initiated.
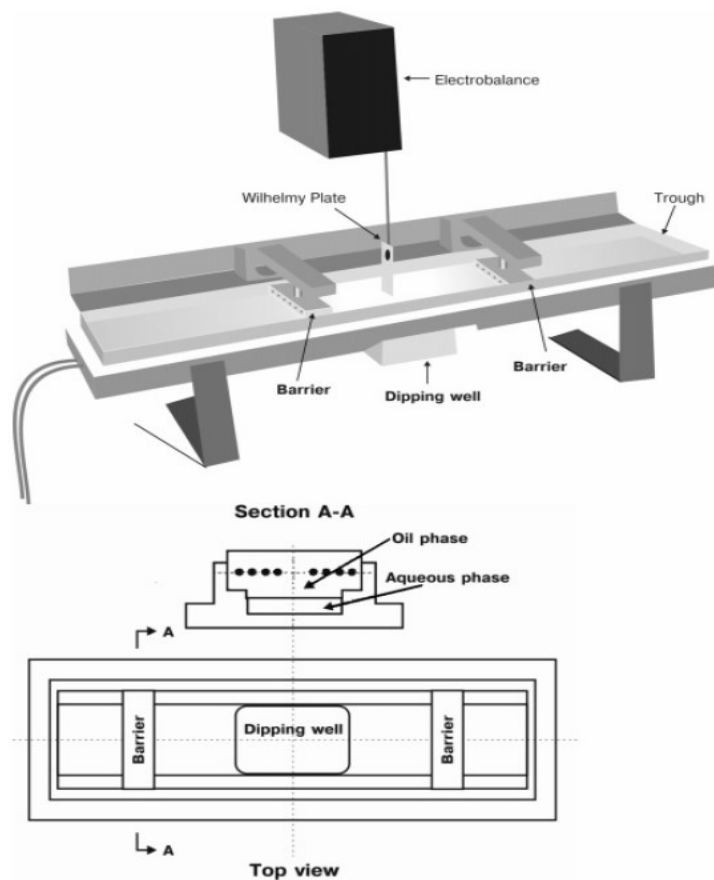
Figure 3.2 Schematic representation of the Langmuir interfacial trough.[103]

A reference isotherm was also collected at a clean water-xylene interface. The pressure measured at a clean water-xylene interface was 11 mN/m, with negligible (< 0.1 mN/m) dependence of the interfacial pressure on the trough area

33

(170 cm^2 to 12.5 cm^2). All experiments were conducted at room temperature (~ 23 °C), and the interfacial films were compressed at a constant rate of 10 mm/min for each barrier, following a previously published procedure.[103]

3.2.5.   Brewster angle microscopy (BAM) imaging

A BAM was used to visualize in situ morphology of interfacial films, see Figure 3.3. One advantage of this technique is that the films could be imaged without drying or disturbing them. In this technique, the water-xylene interface is illuminated by a p-polarized light under Brewster angle (θ_B). At this angle, no light is reflected to the detector and thus the image appears black. The formation of interfacial films modifies the Brewster angle condition, light reflection occurs and the interfacial films will be observed. Further details about this technique and its application to imaging liquid-liquid interfaces can be found elsewhere.[104,105]
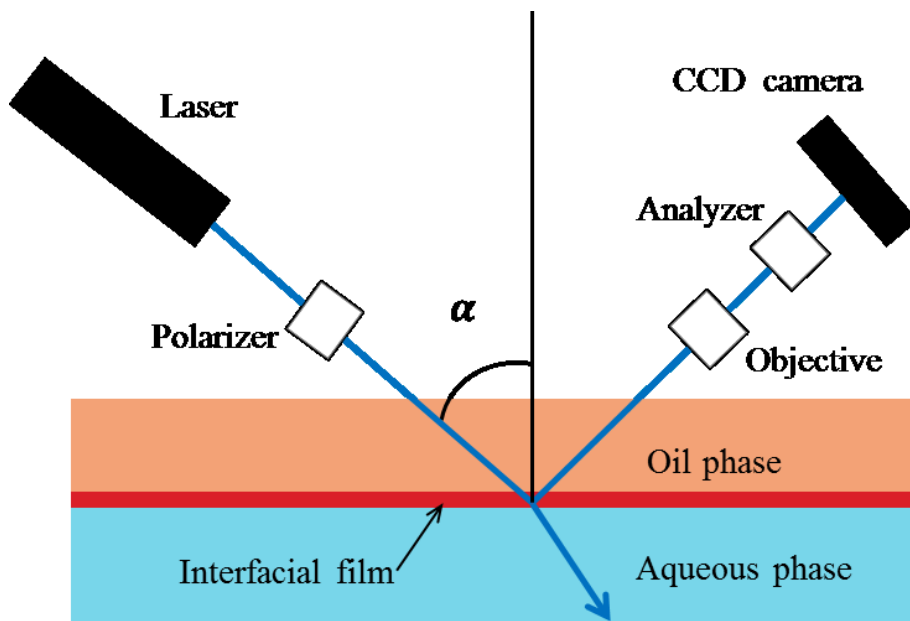
Figure 3.3 Schematic diagram of the BAM setup.

The BAM (Model EP3, Accurion GmbH, Germany) used in this study was modified by Accurion to image liquid-liquid interfaces by addition of light guides,

which were inserted in the top phase to allow the laser beam to reach the interface and reflect back to the photodiode. The optical magnification used was 5×. Images were recorded by a CCD camera and processed using the EP3View2.3× software (Accurion GmbH, Germany). The trough used for these experiments had a fixed area of 28 cm^2, at which all images were collected. First added to the trough was 30 mL of the aqueous phase buffered to pH 4 or 9 as sub-phase. Subsequently 60 mL C5Pe in xylene solutions at the desired concentrations were carefully added on top of the sub-phase as the top-phase. The interfacial films were equilibrated for 30 min before imaging. To calculate the Brewster angle, the refractive index of C5Pe solution and buffer solutions was measured. Based on the Brewster's law: $\tan \theta_B = \frac{n_2}{n_1} = \frac{1.332}{1.497}$ (n_1 is the refractive index of top-phase, and n_2 is the refractive index of sub-phase), the theoretical Brewster angle for the current system is 41.7°. The experimentally found Brewster angle using BAM calibration is 42.0°. The polarizer and analyzer were automatically adjusted to 2° and 10°, respectively. The brightness of the images was adjusted by changing gain values when the images became too bright to see any structure.

This technique is also very sensitive to the thickness of the films: the thicker, the film, the more light, it reflects.[106] Thus, regions with a thicker film are observed as white, while regions with thinner films are seen as gray, and finally, the low-density or almost uncovered sub-phase regions are black.[106] In addition, the refractive index changes when the film forms at the oil-water interface. The computational model could simulate the intensity of reflected light as a function of film thickness in a range of a minimum and a maximum of the refractive index of the film. It should be noted that the smaller difference in refractive index between the oil and water, compared to that between water and air, means that the intensity of the reflected beam due to the presence of an adsorbed film is lower at the water-oil interface.[104] Moreover, the entire oil phase would be illuminated due to the fluorescent properties of model compound C5Pe, increasing the difficulty to position the light at the oil-water interface.

3.2.6.   Langmuir-Blodgett film deposition

Langmuir-Blodgett (LB) films of C5Pe at water-xylene interfaces were deposited on hydrophilic silicon wafers placed parallel to the barriers. Before LB deposition, the wafers were cleaned through sonication in a mixture (1:1) of toluene and acetone for 30 min, followed by soaking in 1M HCl solution for an additional 15 min. The C5Pe films were formed using the procedure described in the previous paragraph (cf. Section 3.2.4.). Then the compression of the films was carried out with a barrier speed of 5 mm/min. Once the target area 130 cm^2 was reached, the films were transferred onto the silicon substrates. The interfacial pressure was kept constant while pulling the wafers up through the water-xylene interface at a speed of 1 mm/min.

3.2.7.   Atomic force microscopy (AFM) imaging

Images of LB films transferred onto silicon wafers were obtained using an Agilent 5500 atomic force microscope (Agilent Technologies, Inc., USA) operating under AC mode in air at room temperature (20 °C). Figure 3.4 shows the schematics of LB film deposition and AFM imaging. The substrates were fixed by a piece of double-sided tape on a sample platform, which was magnetically held in place on the AFM sample stage. Silicon cantilevers (ACT-200, Applied NanoStructures Inc., USA) with a nominal resonance frequency of 200 – 450 kHz and nominal spring constants of 25 – 75 N/m were used for imaging at a scan rate of 1 Hz. Auto tuning was used to determine the resonance frequency of each cantilever used, and the oscillation frequency was set slightly below the actual resonance frequency, such that the probe tip taps gently on the surface. At the beginning, the amplitude was set at 98% of the free amplitude. The amplitude was then compared to the set point, and the resulting difference or error signal was fed into the proportional–integral–derivative (PID) controller, which adjusts the z-piezo, i.e., the probe–sample distance, accordingly.[107] The vendor-supplied SPM software was used to control the probe and scan the sample. The roughness (S_q)

was determined from AFM images using Picoimage basic v. 5.1 software (Agilent Technologies Inc.), according to:

$$S_q = \sqrt{(Z - \bar{Z})^2/N}$$ (3.2)

where N is the number of points analyzed, Z is the height of each point and $\bar{Z}$ is the average height of the N points.

(a)   (b)
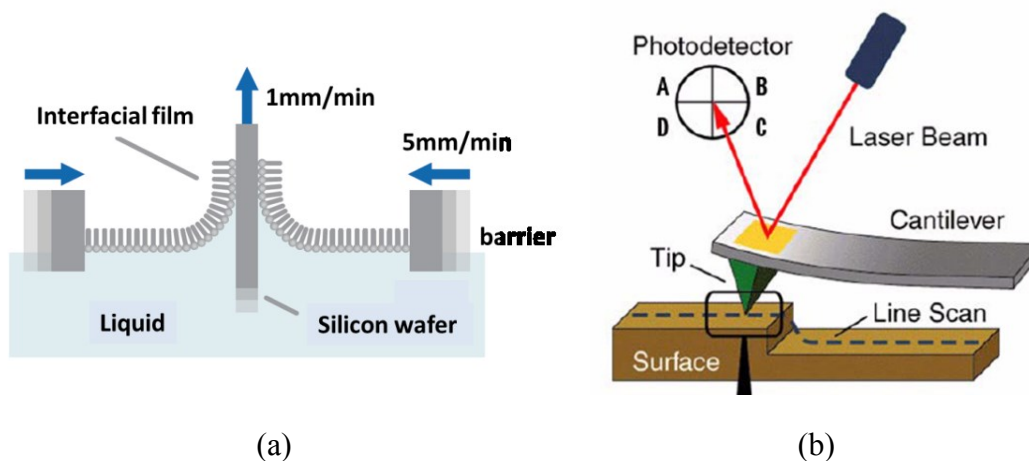
Figure 3.4 Schematics showing: (a) LB film deposition[108]; (b) AFM imaging[109].

3.2.8. Crumpling ratio measurements

When a rigid film is formed at the interface due to irreversible adsorption of surface-active materials, crumpling will be observed during interfacial area reduction. In the absence of irreversible adsorption, the interface will keep fluid and flexible during interfacial area reduction. Crumpling ratio[68,69] was determined using the Pendant drop apparatus (Section 3.2.2.) to qualitatively evaluate the degree of skin formation and elasticity. Higher crumpling ratio indicates a more rigid film.

A water droplet of ~ 10 μL in 0.2 mM C5Pe solution was aged from 5 min to 5 hrs before the droplet was slowly retracted until the whole droplet was withdrawn

into the syringe. A slow rate of contraction was maintained to minimize any droplet vibration that could potentially detach the droplet from the needle tip. The crumpling ratio was determined by analyzing droplet shape images using the instrument provided software.

Chapter 4　　Effect of concentration on interfacial properties of C5Pe

In this chapter, the interfacial behavior of model compound C5Pe at water-oil interfaces was characterized by interfacial tension, interfacial shear rheology, and Langmuir trough experiments, complimented by in situ imaging of the water-oil interface morphology using BAM and AFM imaging of LB films transferred onto silicon wafers. Such a systematic study at water-oil interfaces provides a unique opportunity to relate the mechanical properties of the interfacial films to its morphology and to evaluate the capability of different interfacial techniques to characterize emulsion and film stability.

The interfacial behavior of the model compound was measured under alkaline conditions ensuring that the system is relevant to the industrial process[5,110] and the experimental data can be compared to the behavior of asphaltenes at an equivalent pH.

4.1. Emulsion stability

The interfacial properties of model compound C5Pe were studied in relation to their capacity to stabilize W/O emulsions. An extensive study on emulsion stability was not conducted because similar work was previously performed by Nenningsland et al.[98] The percentage of separated free water was used as an indicator to evaluate the stability of the emulsion.

The effect of C5Pe concentration on emulsion stability is shown in Figure 4.1 for the aqueous phase buffered at pH 9. At low C5Pe concentration (0.005 mM), the emulsion was shown to be very unstable, collapsing almost immediately after emulsification. The initial separated water after emulsification was 37 % and all water separated within 10 min. Increasing C5Pe concentration slightly to 0.01 mM, water separation slowed down although all of the emulsified water separated

39

after 24 hrs. At 0.03 mM C5Pe in xylene, the emulsion stability was dramatically increased with only 13 % separated water after settlement of 24 hrs. Emulsions prepared with higher C5Pe concentrations (0.06 mM and 0.2 mM) were completely stable without any measurable separation of free water. These results are in reasonable agreement with previous findings of Nenningsland et al.[98] with a critical stabilizing (W/O emulsion) C5Pe concentration measured at 0.08 mM, although the authors conducted their study at pH 8. When varying the pH of the aqueous phase the authors observed a stable emulsion prepared using 0.06 mM C5Pe in xylene at pH 9, in good agreement with the current study.
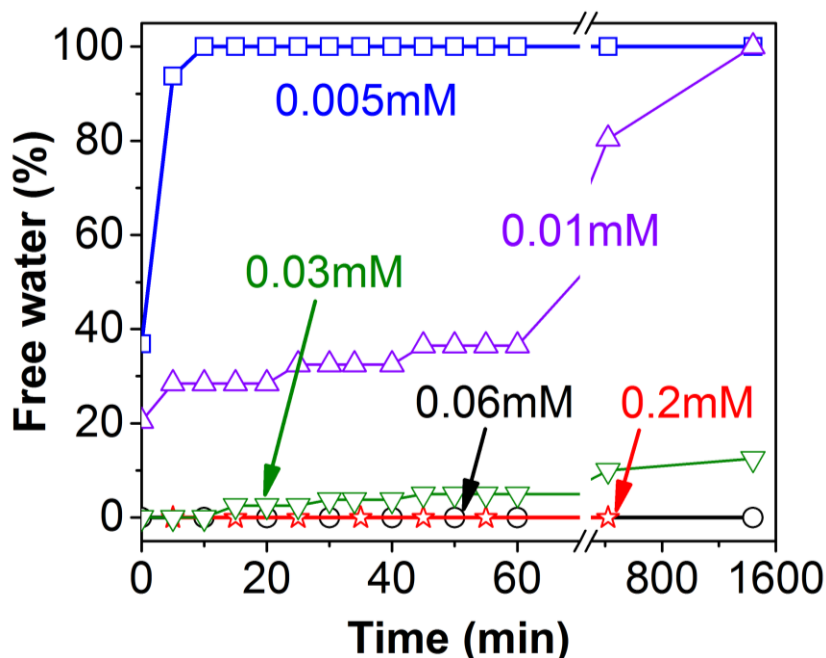

Figure 4.1 Separated free water as a function of time for different concentrations of C5Pe in xylene at pH 9.

4.2. Interfacial properties

4.2.1. Interfacial tension and Langmuir compressional isotherms

The interfacial tension of C5Pe at the water-xylene interface is shown in Figure 4.2a. The concentration of C5Pe solutions varied from 10^{-4} to 0.1 mM and the pH

of aqueous phase were kept at 9. For highly diluted solutions, the interfacial tension decreased slowly with increasing C5Pe concentration. As the solution becomes more concentrated above 1×10^{-3} mM, a sharp reduction of interfacial tension was observed. With a further increase of C5Pe concentration to 0.06 mM, the curve reached value close to zero. Higher concentrations of C5Pe were not measured due to the extremely low interfacial tensions and difficulties in forming a droplet at the needle tip. The equilibrium interfacial tensions (above 0.03 mM) were determined by linear extrapolation from curve γ on $1/\sqrt{t}$ (dynamic interfacial tension data)[111].

The linear regression of data presented in Figure 4.2a can be analyzed with Gibbs equation (equation 4.1) to calculate the maximum adsorption of C5Pe Γ_{max} at interface. For a two component system where solute is ionized,

$$\frac{-d\gamma}{RT} = 2\Gamma_B dlnc_B \tag{4.1}$$

where Γ_B represents the excess solute per unit area at the interface, c_B is the solute concentration, R is gas constant, T is temperature, and γ is interfacial tension. At pH 9, Γ_{max} for C5Pe at water-xylene interface is equal to 1.68×10^{-6} mol/m^2.The area per molecule A_i could be calculated using equation 4.2,

$$A_i = \frac{1}{\Gamma_{max}N_A} \tag{4.2}$$

where N_A is the Avogadro's constant. Substitution of Γ_{max} (1.68×10^{-6} mol/m^2) results in an area per molecule equal to 0.99 nm^2.

A previous study[96] confirmed that the area per molecule of C5Pe in the flat-on arrangement (parallel to the interface) is larger than 1.5 nm^2, and A_i = 0.6 nm^2 when the molecule is configured in the head-on arrangement (perpendicular to the interface). The value 0.99 nm^2 is in-between the two opposing configurations, suggesting a slightly tilted configuration of the aromatic core with respect to the interface. This observation is in good agreement with a mean molecular area of

1.1 nm^2 determined from NMR analysis of emulsions prepared at equivalent conditions.[96]
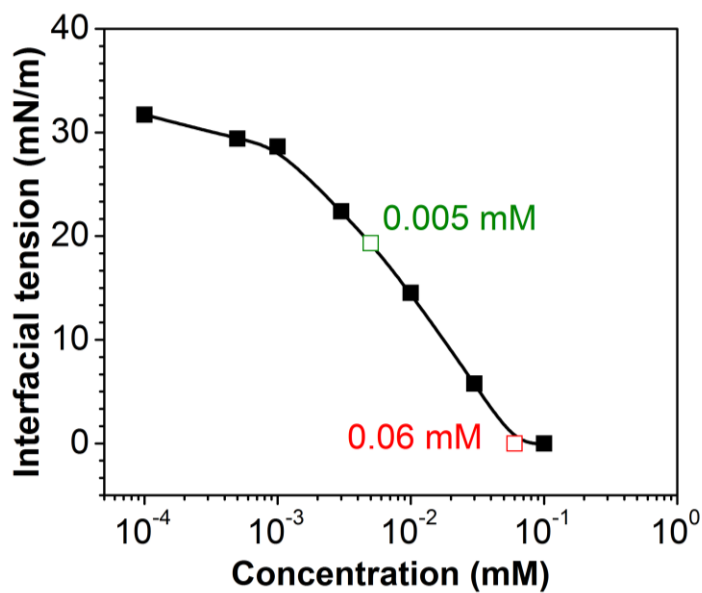
(a)
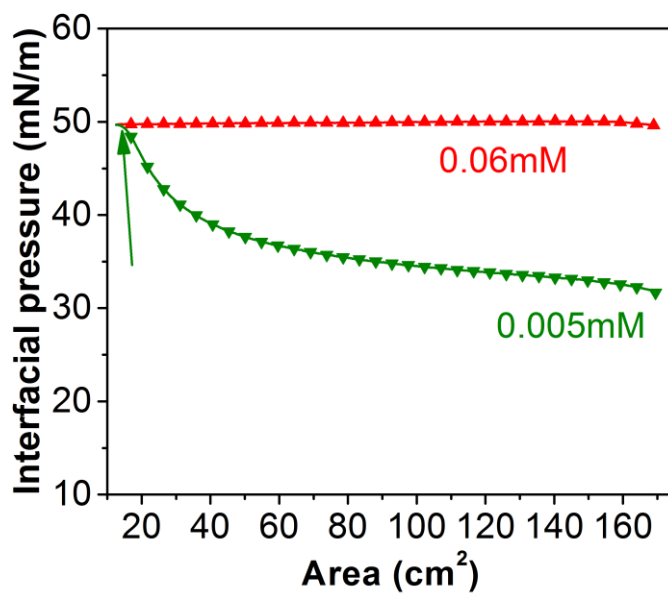
(b)

Figure 4.2 (a) Interfacial tension isotherm of C5Pe dissolved in xylene at the water-oil interface (pH 9), (b) Langmuir compressional isotherms obtained with 0.005 mM and 0.06 mM C5Pe in xylene at corresponding conditions.

The compressional behavior of C5Pe films at an oil-water interface was studied by Langmuir trough. Compression is one mode of deformation at an interface and has been historically studied to shed-light on the mechanism of emulsion stability.[71-73] The π-A isotherms of C5Pe films formed at the water-oil interface using two different C5Pe concentrations in xylene are shown in Figure 4.2b.

Addition of C5Pe to xylene resulted in an interfacial pressure increase at the maximum trough area (170 cm^2) compared to a C5Pe free xylene-water interface (11 mN/m, cf. Section 3.2.4). The measured interfacial pressures before compression at both C5Pe concentrations (0.005 mM and 0.06 mM) are in good agreement with the equilibrium interfacial tensions as measured by the Pendant drop method, see colored open symbols in Figure 4.2a. For 0.06 mM C5Pe in xylene, the change in interfacial pressure was quite small as the interfacial area is reduced from 170 cm^2 to 12.5 cm^2. The high interfacial pressure (~ 50 m/Nm) equates to an extremely low interfacial tension, potentially leading to full interfacial coverage of C5Pe molecules at maximum trough area, hence there is no clear crumpling or rupturing of the interfacial film. A high interfacial pressure and negligible variability under compression relates to an emulsion that is extremely stable, see Figure 4.1. For 0.005 mM C5Pe in xylene, the compressional behavior is considerably different. At maximum trough area, the interfacial pressure equals 32 mN/m and the interfacial pressure gradually increases with a reduction in interfacial area. The interfacial pressure plateaus (identified by green arrow) at 15 cm^2 when the interfacial pressure equals 49.5 mN/m, which corresponds to a closely packed state, as seen for 0.06 mM C5Pe at fully opened trough area (Figure 4.2b). A 91 % reduction in the interfacial pressure before eventual plateau indicates that the water-xylene interface is poorly occupied by the C5Pe molecules at this C5Pe concentration; hence there is little resistance to droplet-droplet coalescence and the formed emulsions separate within a few minutes (see Figure 4.1).

4.2.2. Interfacial shear rheology

The stability of water-in-petroleum oil emulsions is often considered to result from the continual accumulation of asphaltene molecules at the water-oil interface, forming a "protective skin" that resists droplet coalescence.[20-22] The mechanical properties of those skins can be measured by interfacial rheology.

The interfacial shear rheology of C5Pe molecules adsorbed at the water-xylene interface was measured for different initial bulk concentrations (0.005 mM, 0.2 mM, 0.5 mM and 0.725 mM). For all concentrations, Figure 4.3a shows the development in both the viscous (G") and elastic (G') moduli as a function of interfacial aging time. At short aging time the interface exhibits a viscous dominant microstructure with G" > G'. Continual accumulation of the C5Pe molecules at the water-xylene interface leads to an increasing viscous contribution. In addition, continued aging of the interfacial film results in the development of an elastic component. The elastic modulus continues to develop and eventually exceeds the viscous modulus as the film transitions from viscous dominant to elastic dominant microstructures; the exception here is 0.005 mM C5Pe in xylene where the interface remains viscous dominant over 6000 s aging. The aging time for G' to exceed G" is shown in Figure 4.3b. With increasing initial bulk concentration of C5Pe in xylene, the time required to transition from a viscous dominant to an elastic dominant microstructure reduces from 47 min at 0.2 mM C5Pe in xylene to 0 min at 0.725 mM in xylene. It should be noted that the time between sample loading and collection of the first data point takes approximately 1 to 2 min.

In correlating the emulsion stability and interfacial rheology data it becomes apparent that emulsion stability is influenced by the degree of film elasticity. With a viscous dominant film there is little resistance to species mobility, hence breaking down of emulsion is immediate. Elasticity is a rheological property that describes an interconnected network. With continual accumulation of C5Pe molecules at the water-oil interface, a critical concentration is eventually reached

where each individual molecule becomes confined by its neighbors. Restriction to mobility will provide a resistance to film rupture and coalescence. It is not readily apparent whether the critical condition of G' > G'' corresponds to the formation of a 2-D or 3-D film structure, although BAM images to be discussed in Section 4.2.3. most likely support the formation of a 3-D film at the critical condition.
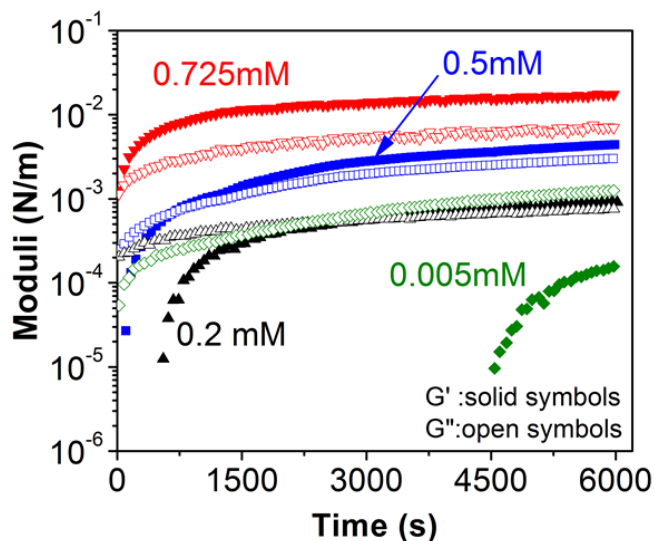
(a)
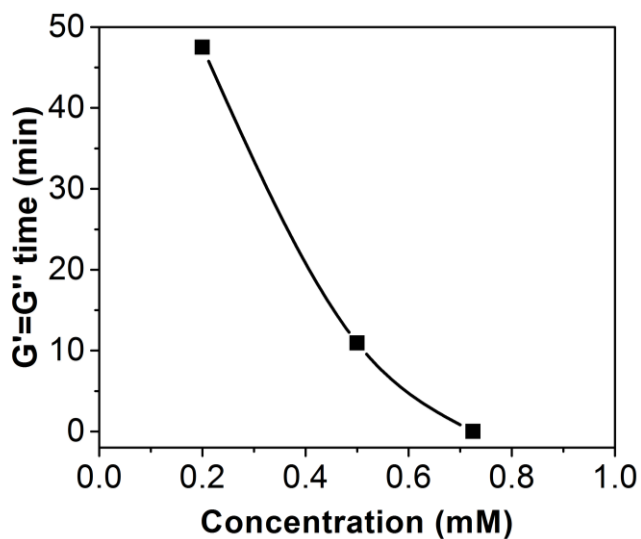
(b)

Figure 4.3 (a) Storage (G') and loss (G'') moduli as a function of aging time as C5Pe molecules adsorb to the water-xylene interface; (b) Critical aging time for G' = G'' as a function of C5Pe initial bulk concentration (water pH 9).

45

Many researchers report highly elastic asphaltene films and attribute the elasticity to a physically cross-linked system.[84,85,112] Frequency sweeps are often considered to determine the gelation kinetics and degree of cross-linking.[113-115] For a pre-consolidated interface, both G' and G" show a strong dependence on the oscillation frequency, when G' < G". After consolidation, G' > G", both moduli show weak dependence on the frequency, proportional to ω^n, with n = 0 – 1.[84] In the current study, frequency sweeps at constant strain (0.8 %) were performed on C5Pe interfacial films aged for 1.67 hrs. Figure 4.4a shows that all interfaces exhibit a weak dependence on the oscillation frequency with the power exponent (n) between 0 and 1 (Table 4.1). There is a clear concentration dependence which confirms that after an equivalent aging time the systems with a higher C5Pe bulk concentration form more consolidated films and a greater degree of film cross-linking.

Table 4.1 G' and G" power exponents (n).

Bulk concentration (mM)	G'	G"
0.2	0.507	0.429
0.5	0.367	0.371
0.725	0.172	0.271

To determine the effect of film consolidation on the mechanical strength of the interfacial film, strain amplitude sweeps at a constant frequency (0.5 Hz) were conducted on the aged interfacial films, see results in Figure 4.4b. In the linear viscoelastic region G' and G" are independent of strain amplitude, implying a coherent microstructure. With an increasing strain both elastic and viscous moduli begin to decrease, eventually transforming from an elastic dominate to a viscous dominate interfacial film. The critical strain is identified as the yield point of the C5Pe interfacial film. For the three elastically dominated films (0.2, 0.5 and 0.725 mM), the yield point was measured at 27.3 %, 55.5 % and 71.7 % strain, respectively (yield point identified by green circles in Figure 4.4b), confirming the formation of stronger interfacial films at higher concentrations of C5Pe in

xylene. This general trend is in good agreement with the emulsion stability data previously discussed.
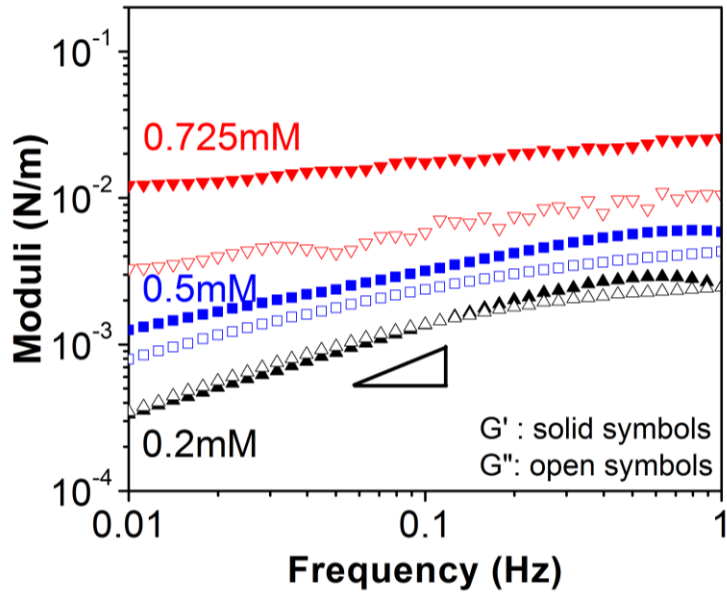
(a)
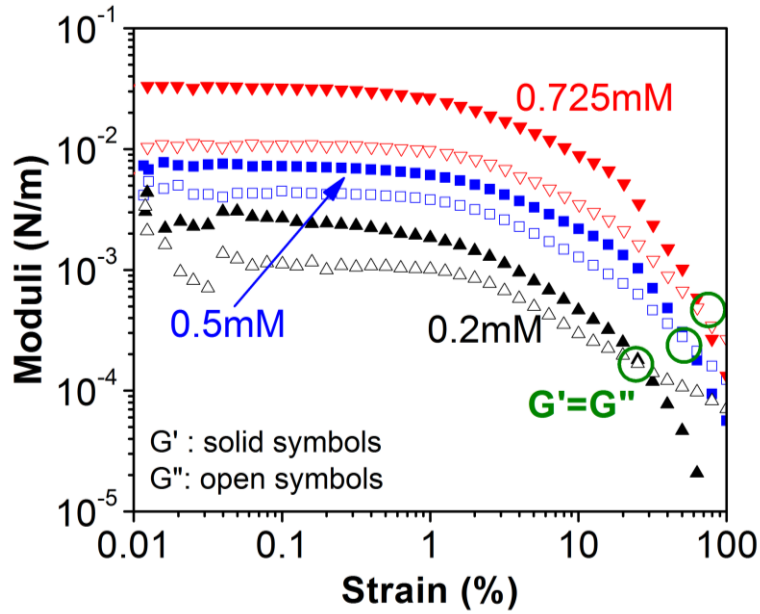
(b)

Figure 4.4 (a) Frequency sweep for water-xylene interfaces stabilized by C5Pe molecules after 6000 s aging; (b) Interfacial film strain sweep as a function of the initial bulk concentration of C5Pe (water pH 9).

4.2.3. Imaging of interfacial layers using BAM and AFM

The shear rheology and compressional isotherms are directly related to the properties of the formed interfacial film. To better interpret the stability data, BAM and AFM images of C5Pe films collected after 30 min aging are shown in Figure 4.5 and Figure 4.6. Initial observations indicate that the structure of the formed film is highly dependent on the initial C5Pe bulk concentration.

| (a) | (b) | (c) |
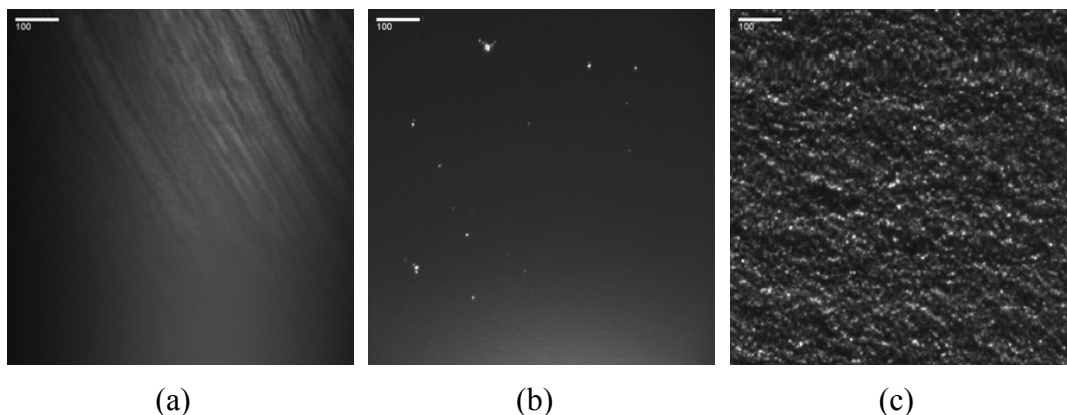
Figure 4.5 BAM images for C5Pe films formed at the water-xylene interface. The aqueous phase is buffered at pH 9, and the concentration increases in the order (a) 0.005 mM; (b) 0.06 mM; and (c) 0.2 mM. (scale bar: 100 μm)

Observations of the interface formed in the presence of 0.005 mM C5Pe in xylene confirmed a very mobile interfacial film. The stripes observed in Figure 4.5a confirm the partitioning of C5Pe molecules at the water-xylene interface, but due to limited coverage the image becomes distorted by the moving film. Film mobility and the absence of a coherent interfacial microstructure would support both the compression isotherm and interfacial shear rheology results. At higher C5Pe concentration (0.06 mM), the film is no longer mobile and appears rigid under video capture. Although not clearly visible in the image, striations in the film begin to develop. In addition, several bright dots appear in the images which imply the formation of C5Pe aggregates at the water-xylene interface. Further investigation of this C5Pe film by AFM confirms an interconnected network of

smaller and larger spherical aggregates corresponding to the striations as observed in Figure 4.6a, with a root-mean-square (rms) roughness of 8.23 nm. The formation of interfacial striations are in good agreement with our previous study wherein the large hydrophobic group and the small hydrophilic head-group of the C5Pe molecules prevent the formation of a uniform monolayer; instead the C5Pe molecules form micelle-like aggregates in the film.[93,94] Further increase in the C5Pe concentration to 0.2 mM led to a thicker film with identifiable surface features as measured by BAM (Figure 4.5c). The film roughness measured by AFM increased to 20.90 nm, see Figure 4.6b.

(a)   (b)
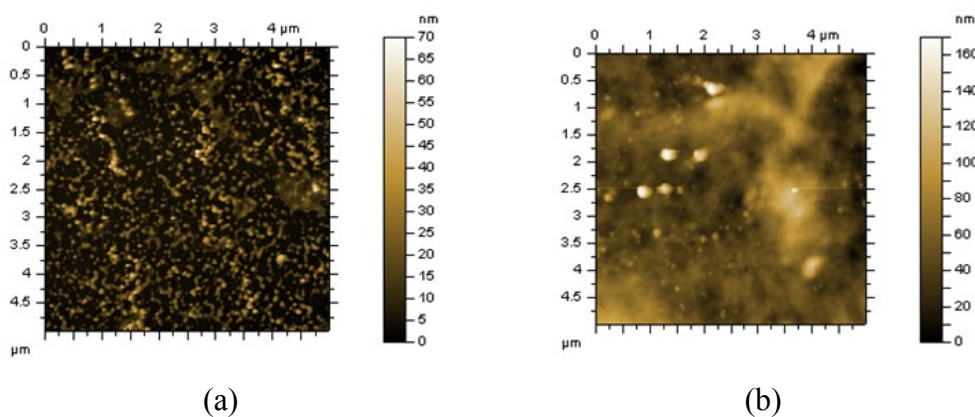
Figure 4.6 AFM images of C5Pe films deposited on silicon wafers: (a) 0.06mM (vertical scale is from 0 to 70 nm); (b) 0.2mM (vertical scale is from 0 to 170 nm). (water pH 9)

4.3. Conclusions

When the aqueous phase is basic (pH = 9), the emulsion stability increased as a function of initial C5Pe concentration. Interfacial tension isotherm confirmed high interfacial activity of C5Pe at pH 9, which results from the deprotonation of −COOH groups. Based on the linear regression in interfacial tension isotherm, the maximum C5Pe adsorption at interface and area per molecule were calculated. The value of A_i suggested that C5Pe molecules arranged at water-xylene interface

with a slightly tilted configuration of the aromatic core with respect to the interface.

The mechanical properties of interfacial films were studied under lateral compression and oscillatory shear. At higher C5Pe concentration, the film exhibited lower compressibility and higher elasticity. The transition from elastic dominant to viscous dominant films was faster. Also, weaker dependence on frequency and larger critical strain were measured at higher C5Pe concentration. The morphology of interfacial films shown in BAM and AFM images is in good agreement with interfacial shear rheology and Langmuir trough results. The thin and smooth film was viscous and compressible, while the thick and rough film yielded high elasticity and high interfacial pressure.

In correlating the mechanical properties and morphology of interfacial films with emulsion stability, it becomes apparent that only the densely-packed, thick films, which equipped with high elasticity and low compressibility, could protect water droplets from coalescence and hence stabilize W/O emulsions.

Chapter 5 Effect of water chemistry on interfacial properties of C5Pe

Research has been conducted using model compounds to elucidate the effect of solvent composition, pH of the aqueous phase and model compound concentration on emulsion stability, as determined with bottle tests. It was found that emulsions were most stable at alkaline pH values and when the oil phase was an aliphatic solvent[98]. While this study provides useful insights regarding the effect of solvent type and water chemistry on the stability of emulsions in the presence of model compounds, it does not correlate the observed changes in emulsion stability with the physical properties of interfacial layers, such as their rigidity and morphology. Wang et al.[94] reported that addition of Ca^{2+} ions promoted the adsorption of C5Pe molecules at the mica surface, causing an increase in the steric repulsion between mica surfaces coated with C5Pe, but the solid-liquid interfaces used in this work are not necessarily similar to liquid-liquid interfaces. It is thus worth further exploring the effect of pH and Ca^{2+} ions on the adsorbed C5Pe molecules at the water-oil interface.

5.1. Effect of pH

5.1.1. Emulsion stability

The effect of pH on C5Pe stabilized emulsion was evaluated by bottle tests. The concentration of C5Pe was kept constant at 0.2 mM and the pH of aqueous phase was buffered at 4, 7 or 9. The results are shown in Figure 5.1.

At pH 4, the emulsion was initially unstable with an amount of 41 % water separated after 25 min settling. Then the curve tended to plateau out, transferring to a stable region. After 24 hrs, the amount of separated water reached 53 %. When the aqueous environment was neutral or basic (pH 7, 9), the emulsions were completely stable and the amount of free water separated over a 24 hrs time

period was negligible. The results showed that high pH facilitates the formation of stable emulsions, agreeing with previous work[98] where the emulsion stability was determined as a function of pH at 0.06 mM C5Pe. It was found that water separated completely after emulsification for pH $\leq$ 6, while the emulsion started to show some stability above pH 7, and no sign of water droplets coalescence was observed at pH $\geq$ 9.[98] The pH dependence of the emulsification properties of C5Pe provides an opportunity to tune the surfactant properties of C5Pe to match the interfacial behavior of the asphaltene sub-fraction of heavy/crude oil by varying the pH of the aqueous phase.
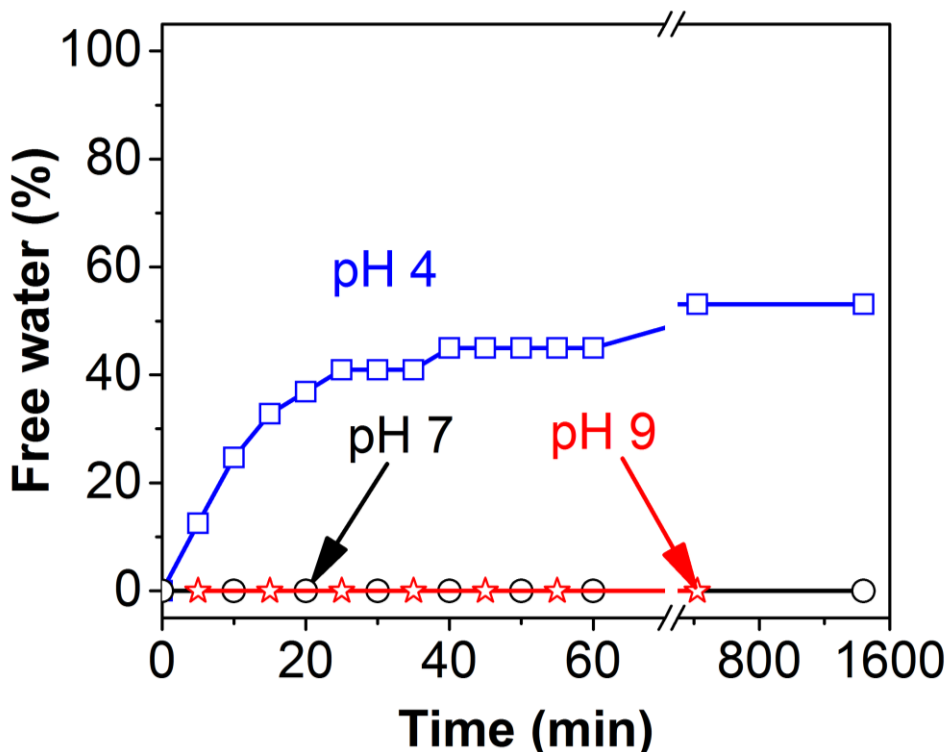
Figure 5.1 Separated free water as a function of time in bottle tests (emulsions were prepared with 0.2 mM C5Pe in xylene at different pHs).

5.1.2. Interfacial tension isotherms

The interfacial tension of C5Pe at the water-xylene interface was measured at pH 4, 7 and 9 (Figure 5.2). At low concentration ($< 1\times10^{-3}$ mM), the pH of aqueous

52

phase does not cause obvious differences in the interfacial tension of C5Pe. It is probably the result of insufficient C5Pe molecules in the bulk oil phase. For concentrations higher than 1×10^{-3} mM, the interfacial tension decreased with increasing pH at a fixed concentration. For pH = 4, the interfacial tension was as high as ~ 17 mN/m, even at the highest concentration studied (0.5mM), while the values of interfacial tension for pH 7 and pH 9 were measured around zero at 0.5 mM and 0.06 mM, respectively.
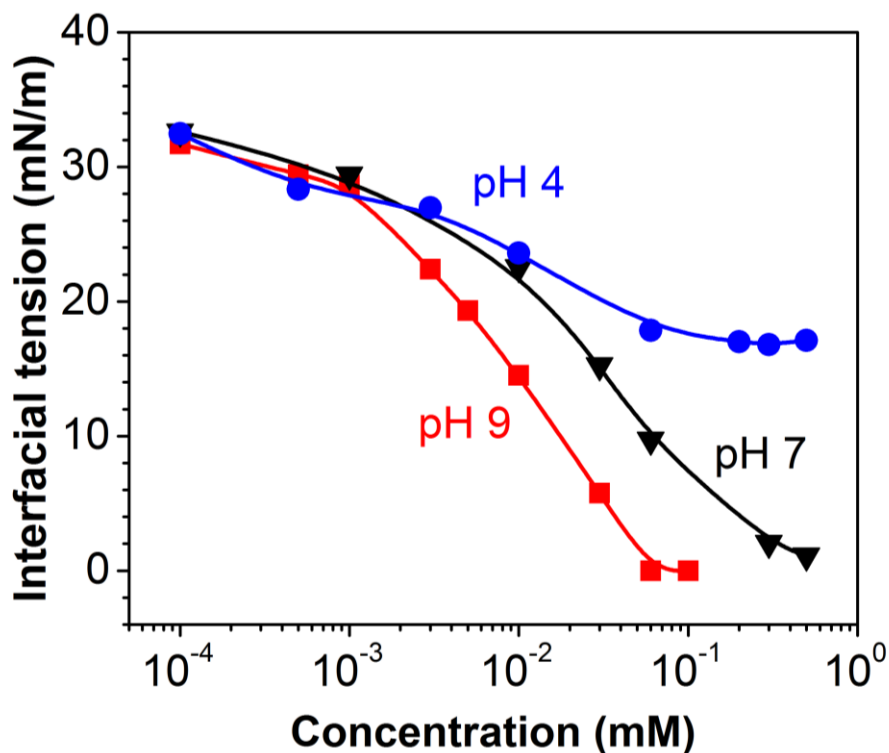
Figure 5.2 Interfacial tension isotherms of C5Pe dissolved in xylene at the water-oil interface (pH 4, 7, 9).

Interfacial tension isotherms showed that the interfacial activity of C5Pe is strongly dependent on pH, which is consistent with bottle test results. At high pH, –COOH groups of C5Pe molecules are deprotonated, C5Pe molecules have high affinity to water-oil interfaces, and thus C5e molecules are driven to accumulate surrounding water droplets to stabilize the emulsion.

The Gibbs equation was also applied to linear regression regions in isotherms at pH 4 (for a two component system where solute is not ionized, $\frac{-d\gamma}{RT} = \Gamma_B dlnc_B$) and pH 7, with the analysis being done in the similar manners as in the case of pH 9 (cf. Section 4.2.1).

For good comparison, the maximum adsorption of C5Pe Γ_{max} at interface and area per molecule A_i in three cases were all listed in Table 5.1. With increasing pH, A_i decreased monotonically, which indicates that the arrangement of interfacial C5Pe molecules is more compact at higher pH. As stated before, $A_i >$ 1.5 nm^2 corresponds to the flat-on arrangement (parallel to the interface), and $A_i <$ 0.6 nm^2 corresponds to the head-on arrangement (perpendicular to the interface). Since A_i in all cases is between 0.6nm^2 and 1.5nm^2, C5Pe molecules were configured in a tilted geometry of the aromatic core with respect to the interface at any studied pH. It is reasonable to claim that the pH of aqueous phase doesn't change the basic orientation of interfacial C5Pe molecules, probably just change the angle of the aromatic core to the interface.

Table 5.1 Maximum adsorption of C5Pe at the water-xylene interface and area per molecule at different pHs.

pH	Γ_{max} mol/m^2	A_i nm^2/molecule
4	1.26×10^{-6}	1.32
7	1.47×10^{-6}	1.13
9	1.68×10^{-6}	0.99

5.1.3. Langmuir compressional isotherms

The compressional isotherms shown in Figure 5.3 were obtained by adding solutions of varying concentrations of C5Pe in xylene on aqueous sub-phase buffered at pH 4. Table 5.2 shows the transition areas (A_t) and transition pressures (π_t).
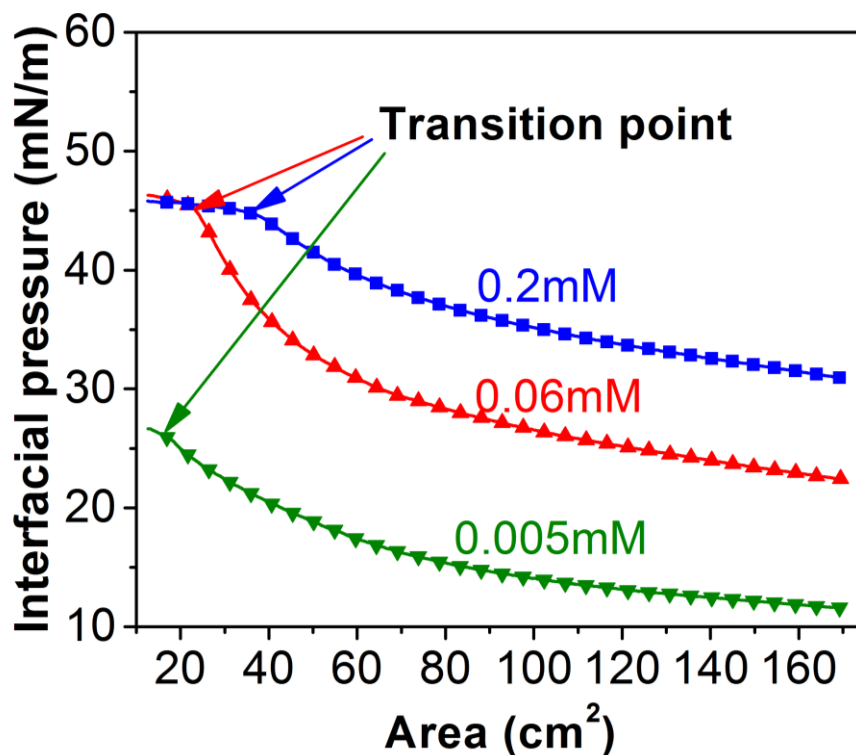
Figure 5.3 Langmuir isotherms obtained at pH 4 with different C5Pe concentrations in xylene.

Table 5.2 Values of areas and pressures at transition points of the compressional isotherms (buffer solution of pH 4).

Concentration (mM)	Transition area A_t (cm^2)	Transition pressure π_t (mN/m)
0.005	18.2	25.6
0.06	24.0	44.7
0.2	38.7	44.4

The transition point here is defined as the point in the isotherm where the slope $(\partial\pi/\partial A)$ starts to decrease. Similar change in slope of compressional isotherms have been reported in previous studies and attributed to either film collapse [116-118] or phase transition from liquid-expanded to liquid-condensed states[119,120]. The

former may occur when the film is restructuring to form multilayers, as has been observed for several polymers.[121]

The interfacial pressure increased with C5Pe concentration at maximum trough area, following the relation described in equation 3.1. Above 0.005 mM, π_t (the interfacial pressure at transition point) was quite high and similar, around 45 mN/m. Their high π_t values revealed that these films packed closely on aqueous phase. The transition points appear to result from film collapse rather than phase transition from liquid-expanded to liquid-condensed. For the lowest solution concentration of 0.005 mM, the transition pressure was low (~ 26mN/m), similar to the value of interfacial pressure at the beginning of compression for 0.06mM C5Pe film. It is therefore reasonable to believe that the film formed with 0.005 mM C5Pe transformed to a condenser phase. In other words, this transition point was the result of phase transition from liquid-expanded to liquid-condensed. In comparison with interfacial films at pH 9 (Figure 4.2b), the films at pH 4 were softer and more compressible. These results support the findings that C5Pe has low interfacial activity and could not form stable emulsions at pH 4.

5.1.4. Interfacial shear rheology

To focus on the effect of pH on the growth of elastic films, the development of elastic modulus (G') as a function of aging time at 0.06 mM and 0.2 mM C5Pe in xylene solutions was shown in Figure 5.4. The development of G' could be divided into two regions regardless of pH and C5Pe concentration. In the first region, G' developed fast. In the second region, G' increased at a slower rate and gradually leveled off. A similar development of G' was reported by Kilpatrick and his co-workers.[66] They attributed the change in G' of asphaltene films with time to two phenomena – adsorption of asphaltenes and molecular rearrangement.[66] Linear increase of G' in the first region corresponds to fast adsorption of C5Pe onto the interface. The slower development of G' in the second region is the result of rearrangement of C5Pe molecules.
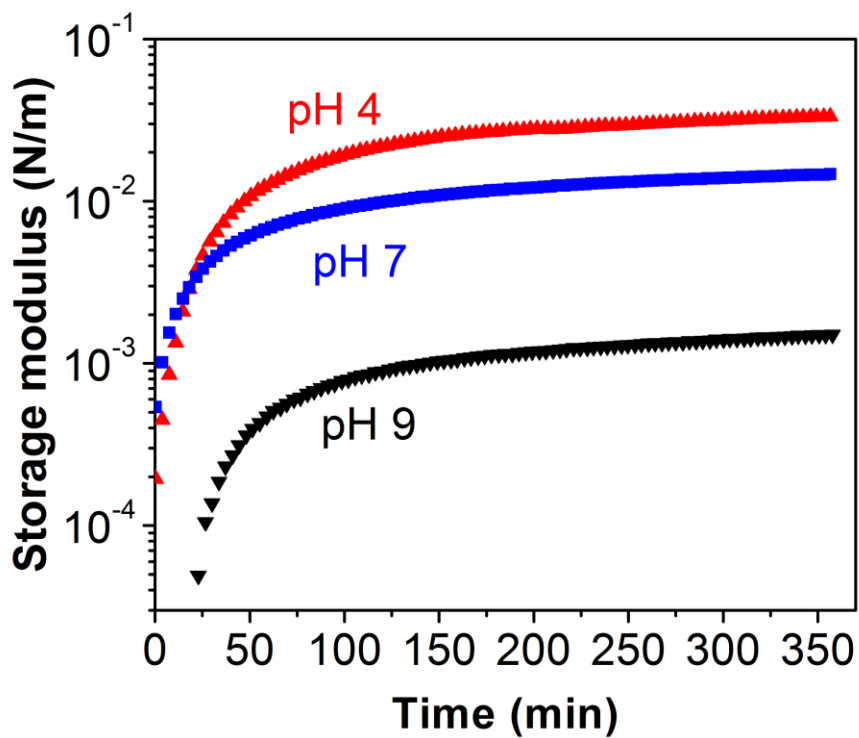
(a)
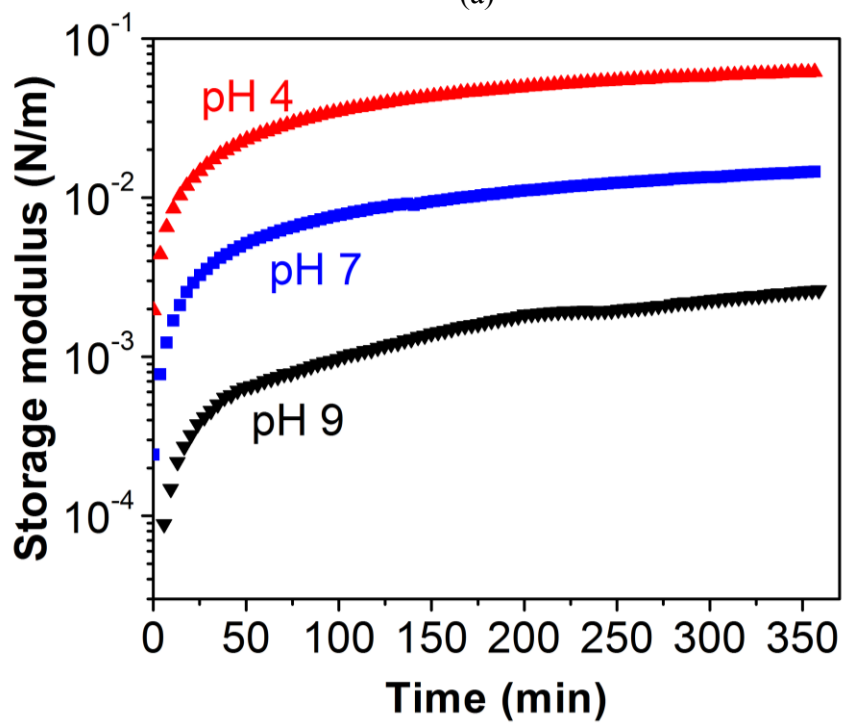
(b)

Figure 5.4 Storage modulus (G') as a function of aging time as C5Pe adsorb at the water-xylene interface with different pHs: (a) 0.06 mM; (b) 0.2 mM.

It is interesting to find that G' got the highest value throughout 6 hrs at pH 4, which is opposite to its lowest emulsion stability. This trend contradicts previous finding that interfacial shear elastic modulus of asphaltene films corresponds well with aged water-in-model oil emulsion stability.[66,122] Unfortunately, we do not have a good explanation for the observed reproducible discrepancy. It is possible that G' is not always a good indicator of emulsion stability under all circumstances. More work is required to understand this phenomenon.
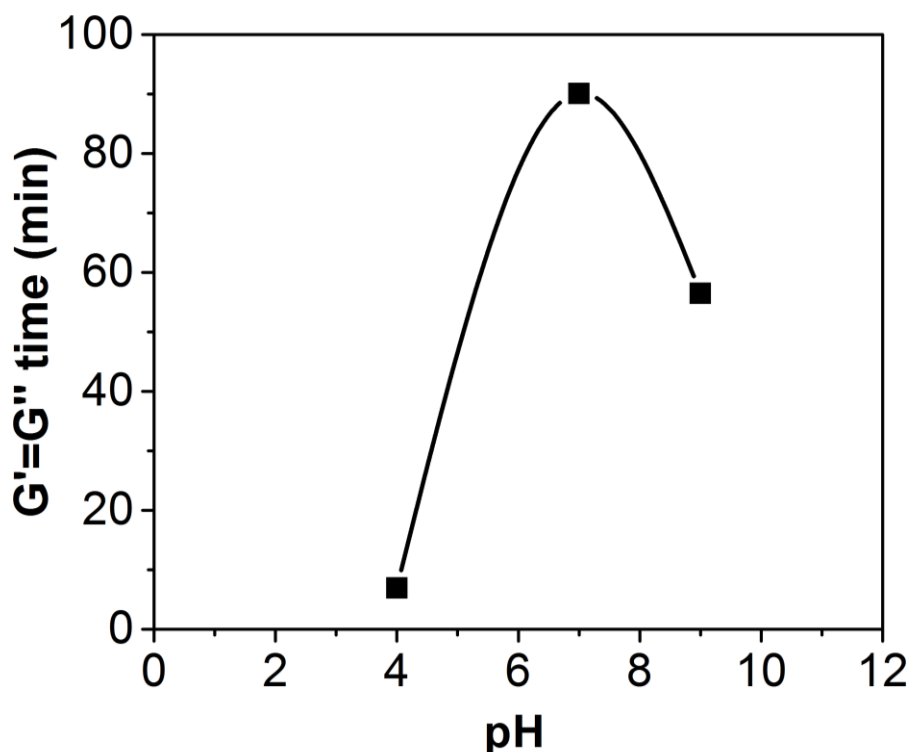
Figure 5.5 Critical aging time for G' = G'' as a function of pH of aqueous phase (0.2 mM C5Pe in xylene).

To further understand the viscoelastic properties of C5Pe films, the time to reach transition condition G' = G'' was evaluated. As shown in Figure 5.5 that the elastic-dominant film formed faster at both low and high pHs. Given pK_a of C5Pe at approximately pH 6,[94] most C5Pe molecules are not ionized at pH 4. In this case, it appears that interfacial C5Pe molecules packed fast through π-π

interaction, without the interference of electrostatic repulsion. In the case of pH 9, the dissociation of carboxylic groups significantly increased the interfacial activity of C5Pe molecules, enhancing their anchor to the interface. The C5Pe molecules irreversibly anchored at the interface, while more C5Pe molecules were driven to migrate from bulk oil phase to the interface, forming an elastic film relatively fast.
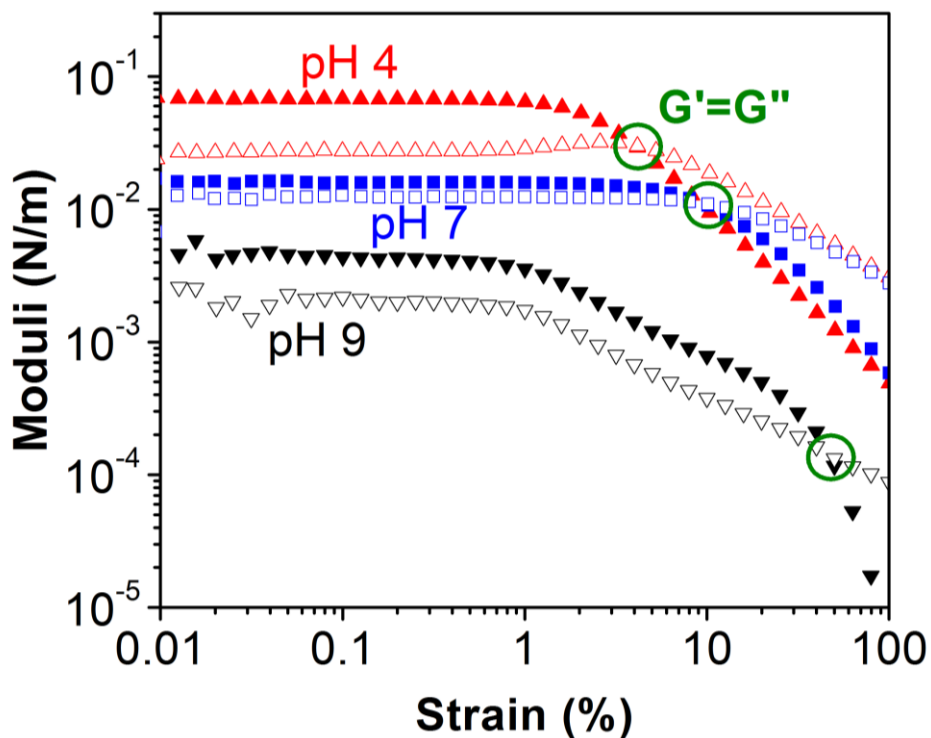
Figure 5.6 Interfacial film strain sweep as a function of pH of aqueous phase (0.2 mM C5Pe in xylene).

At the end of each experiment, strain amplitude sweep was conducted at a constant frequency of 0.5 Hz. The results in Figure 5.6 show that increasing the pH of the aqueous phase from 4 to 9, the critical strain value at the yield point increased from 4.02 % to 46.3 % (yield point identified by green circles). The results reveled that C5Pe-stabilized film at higher pH had higher resistance to deformation. Although the film formed from acidic aqueous phase showed high elasticity, it was more fragile and little force would rupture it. Therefore water

59

droplets protected by these films readily coalesce, leading to unstable emulsion. It seems that high mechanical strength rather than high elasticity of interfacial films correlates well with emulsion stability.

5.1.5. Crumpling ratio

Langmuir trough experiments provide information on film deformation under lateral compression. Interfacial shear rheology studies the deformation of the films by applying shear to a constant interfacial area. Crumpling ratio measurement is another method to investigate the deformation of interfacial films. In this technique, the film is subjected to compression from all directions by volume contraction. Thus, these three methods probe the mechanical properties from different aspect, and they complement each other to make a comprehensive evaluation of the films.
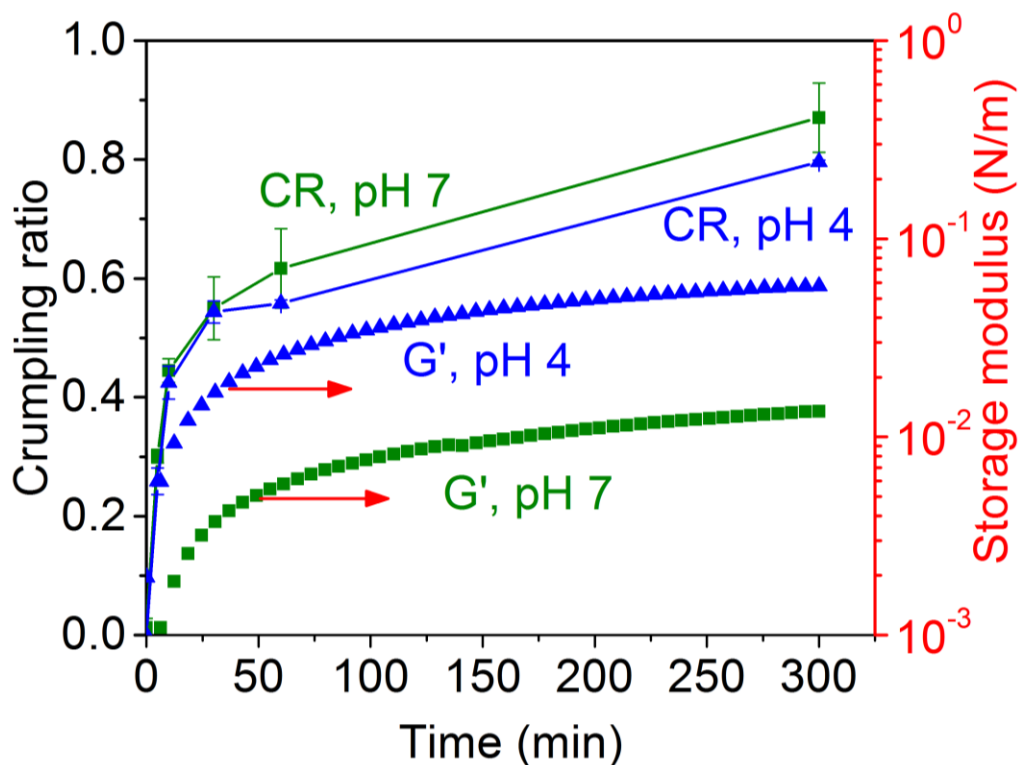
Figure 5.7 Measurement of droplet crumpling ratio and interfacial shear elasticity (G') as a function of interfacial aging time.

To better understand the phenomenon that film elasticity (G') was highest at pH 4 (Figure 5.4), crumpling ratio measurements were conducted at corresponding C5Pe concentration (0.2 mM). Due to low interfacial tension, it is impossible to hold water droplets at pH 9. Here, the interfacial elastic modulus and crumpling ratio were compared at pH 4 and pH 7 in Figure 5.7. Data points represent the average of a minimum of 5 measurements for short aging time, 3 measurements for long aging time (5 hrs) with the error bars reporting the standard deviation. At short aging time, crumpling ratio increased fast, despite of the pH of aqueous phase. The increase of crumpling ratio slowed down in both cases after aging of ~ 30 min. Similar trend was observed in development of G'. G' became flattened out after initial fast increasing over the same time region. With 300 min aging, the average crumpling ratios at pH 4 and pH 7 were 0.80 and 0.87, respectively. The high crumpling ratios validated the high elasticity of the films formed at acidic

and neutral aqueous conditions observed in Figure 5.4. The results showed a good agreement between crumpling ratio and interfacial shear rheology in characterization of film rigidity. Meanwhile, the irreversibility of C5Pe adsorption at the water-oil interface was confirmed in Figure 5.7.

5.1.6. Imaging of interfacial layers using BAM and AFM

The morphology of film built from 0.2 mM C5Pe on aqueous phase of pH 4 was shown in Figure 5.8. The morphology was totally different from that at basic condition, where a complex 3D structure was formed, as shown in Figure 4.5 and Figure 4.6.

(a)   (b)
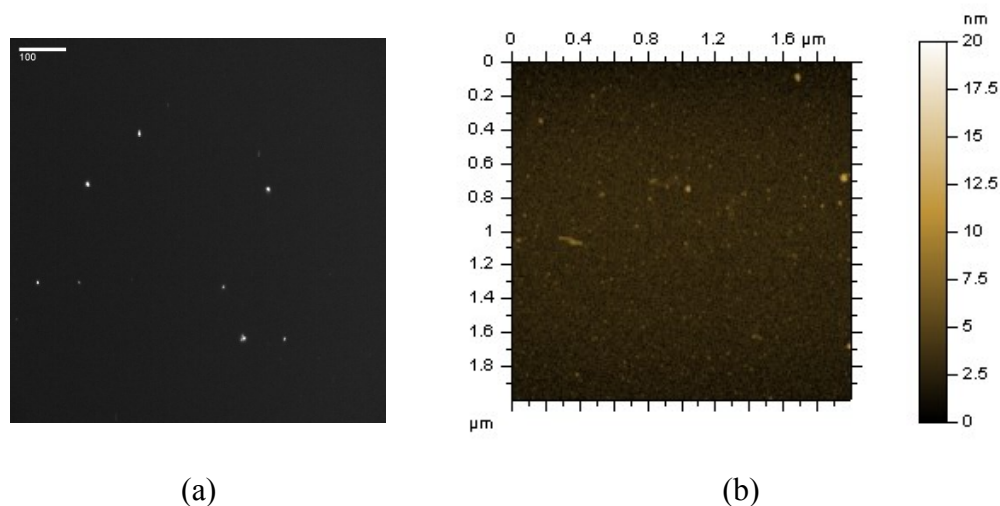
Figure 5.8 BAM (a) and AFM (b) images for 0.2 mM C5Pe film formed at the water-xylene interface. (aqueous phase: pH 4; BAM scale bar: 100 μm).

At pH 4, the film was quite flat with several spherical aggregates, see Figure 5.8a. The black background in the image probably indicates that the film was quite thin at this condition. Imaging at higher resolution is required to better visualize the film features at the interface. Thus, the morphology of this film was scanned by AFM in 2×2 μm (Figure 5.8b). Many tiny dotted aggregates were observed in this film, and the rms roughness was 0.65 nm. In comparison with the film prepared with identical C5Pe concentration at pH 9 (Figure 4.6), the size of aggregates is significantly smaller and the surface is much smoother. Although the films at

acidic condition were not as compact as those at basic condition, some small aggregates did form at interfaces, which could resist coalescence of water droplets to a certain extent. As a result, the emulsions at corresponding condition did not completely break after settling for 1 day.

5.2. Effect of calcium ions

As shown in Figure 5.9, the effect of calcium ions on shear rheological properties of C5Pe films were studied under both acidic and basic conditions. Figure 5.9a shows the effect of Ca^{2+} on viscoelastic properties (G', G'') of 0.06 mM C5Pe films at basic condition. At Ca^{2+} concentrations below 0.1mM, Ca^{2+} had a negligible effect on the rheological properties of viscosity-dominated C5Pe films. An increase of Ca^{2+} concentration to 0.1mM significantly accelerated the formation of interfacial films dominated by elasticity. G' rapidly increased with time and exceeded G'' after 11.1 min of aging, implying that the film transformed from viscous dominant to elastic dominant. After 6 hrs aging in the presence of 0.1 mM Ca^{2+}, G' was one order of magnitude greater in comparison with C5Pe film without addition of Ca^{2+}. When the concentration of Ca^{2+} was higher than 0.1 mM, interfacial films behaved similarly. The elastic dominant film formed so fast that the transition was not observed by showing G' greater than G'' within 6 hrs.

(a)

(b)

Figure 5.9 Effect of Ca^{2+} on viscoelastic properties of C5Pe films at the water-xylene interface: (a) 0.06 mM C5Pe (pH = 9); (b) 0.2 mM C5Pe (pH = 4).
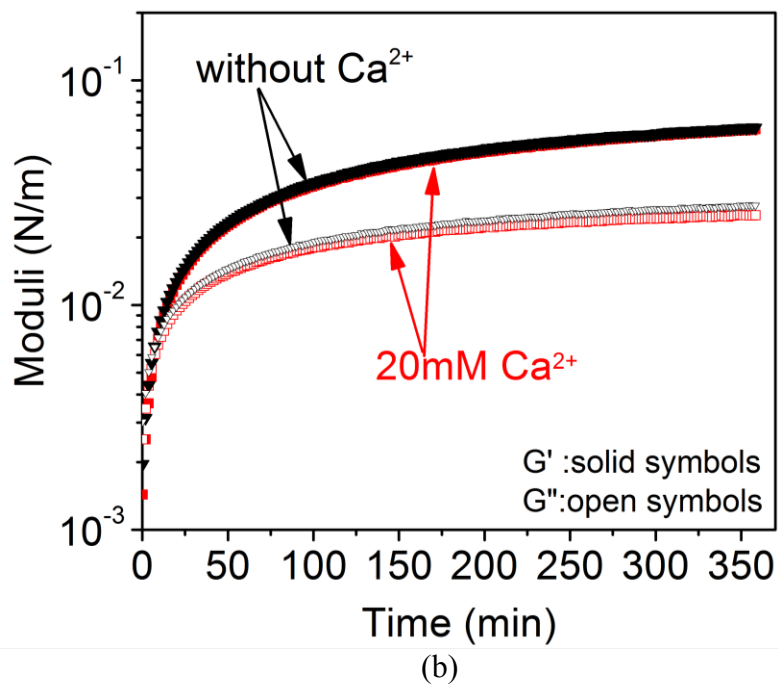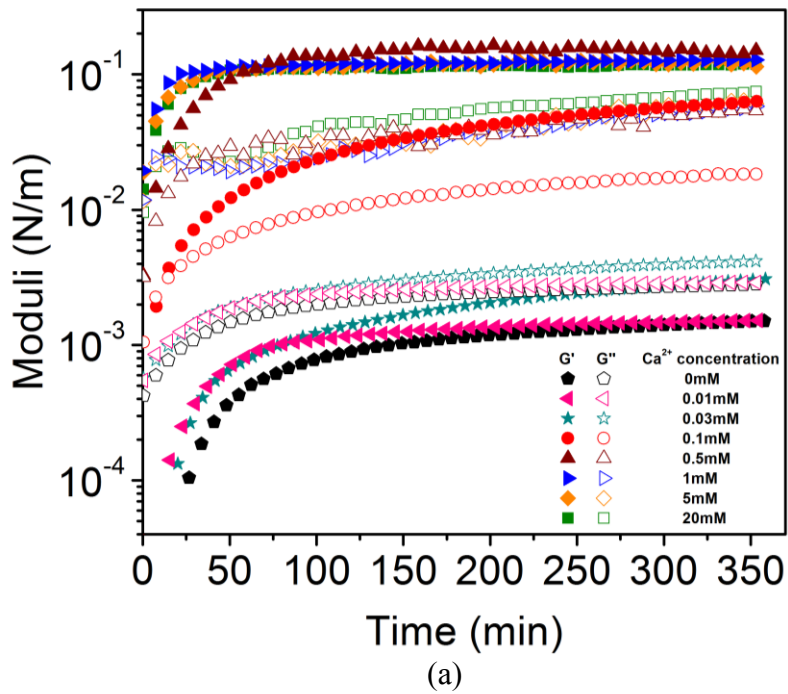
The results showed that film elasticity increased with the presence of Ca^{2+} ions, indicating Ca^{2+} ions could rigidify the interfacial films. Previous study found that

the thickness of C5Pe films increased with Ca^{2+} addition and attributed it to further aggregation of C5Pe induced by Ca^{2+} ions through bridging binding with the –COOH head groups.[94] The formation of bigger aggregates at water-oil interfaces appears to contribute to the increased film elasticity.

The results in Figure 5.9b shows that Ca^{2+} ions had no impact on viscoelastic properties of C5Pe films at pH 4, correlating well with low interfacial activity of C5Pe observed in Figure 5.2. The development of G' and G" upon the addition of large amount of Ca^{2+} ions (20 mM) was found to overlap with the curves obtained in the absence of Ca^{2+} ions. Ca^{2+} ions are not able to connect electroneutral C5Pe molecules, leading to the independence C5Pe film growth on Ca^{2+} ions, even at high concentration of 0.2 mM C5Pe.

5.3. Conclusions

The interfacial properties of a polyaromatic surfactant C5Pe was studied in water-xylene system. The results showed that the pH of aqueous phase and Ca^{2+} ions strongly influenced the interfacial behavior of C5Pe molecules. At low pH, C5Pe molecules have low affinity to the water-oil interface by showing high interfacial tension, and their insufficient accumulation at interface leads to smooth and thin interfacial films. These films are compressible and rupture under small strain, resulting in unstable W/O emulsions. At high pH, the ionization of C5Pe molecules completely changed the situation. The densely-packed, rough films of high mechanical strength formed and prevented water droplets from coalescing, thus leading to stable W/O emulsions. An interesting finding was that the highest film elasticity (G') was measured at pH 4, where the stability of emulsion was lowest. The crumpling ratio at low pH agrees well interfacial shear rheology results, confirming the high rigidity of interfacial films. Considering that the values of critical strain (representing the mechanical strength of interfacial films) were higher at higher emulsion stability, critical strain rather than G' seems to be better indicator of emulsion stability, at least in this case. It was also found that

Ca^{2+} ions rigidified C5Pe films by binding C5Pe molecules together through interactions with charged –COOH groups of C5Pe molecules at high pH.

Chapter 6   Summary

6.1. General conclusions

This thesis focuses on investigating the interfacial properties of an asphaltene model compound C5Pe, in an attempt to understand the correlation between interfacial behavior and emulsion stability. A systematic study on the impact of C5Pe concentration and water chemistry is presented. The conclusions of this study are summarized as follows:

1. Interfacial shear rheometer (ISR), incorporating with Langmuir–Blodgett trough and crumpling ratio measurement, has been shown to be a powerful approach to study the mechanical properties of interfacial films.

2. The stability of C5Pe-stabilizied emulsions corresponds well with the properties of interfacial films, which depend strongly on their concentration, pH of the aqueous phase and Ca^{2+} addition.

3. Due to ionization of the carboxylic groups, C5Pe exhibited high interfacial activity at basic condition (pH 9). Thus stable emulsions are produced when an adequate amount of C5Pe is adsorbed at the water-oil interface. Results from ISR and Langmuir trough showed that the interfacial layers formed from high C5Pe concentration are substantially more elastic and rigid. The thicker and rougher C5Pe films observed in BAM and AFM images are in line with their mechanical properties and emulsion stability at corresponding conditions, indicating that C5Pe stabilizes W/O emulsions through the formation of thick films.

4. At acidic condition (pH 4), C5Pe molecules have low affinity to the water-oil interface, and hence insufficient accumulation at interface leads to smoother and thinner films. These films are compressible and deformable, yielding low resistance to coalescence of water droplets and hence unstable W/O emulsions.

Ca^{2+} ions are shown to rigidify C5Pe films by binding C5Pe molecules together through interactions with –COOH groups of C5Pe molecules at basic condition.

Table 6.1 The effects of C5Pe concentration and water chemistry on the interfacial properties of C5Pe.

Variables	Interfacial properties	Conclusions
C5Pe concentration (at pH 9)	At higher concentration: lower interfacial tension; higher film elasticity, higher film mechanical strength; lower film compressibility; thicker and rougher films.	The mechanically strong and viscoelastic interfacial films prevent water droplets from coalescence and hence stabilize W/O emulsions.
pH of aqueous phase	At acidic condition (pH 4): higher interfacial tension; higher film elasticity, lower film mechanical strength; higher film compressibility; smoother and most likely thinner films.	At acidic condition, the interfacial films have higher compressibility and lower mechanical strength, which for this system are better indication for W/O emulsion stability.
Ca^{2+} addition	At pH 4, no impact on film viscoelasticity; at pH 9, formation of elasticity dominant film was accelerated.	Ca^{2+} ions rigidify interfacial films by binding C5Pe molecules through interactions with –COOH groups of C5Pe molecules at pH 9.

6.2. Recommendations for future work

To gain a better understanding of interfacial properties of model compound C5Pe and provide valuable insights for industrial process, following can be conducted.

1. In this study, the pH of aqueous phase and Ca^{2+} addition showed a strong influence on interfacial properties of C5Pe. However, a systematic study is required to further investigate the effect of water chemistry, such as ionic strength and other cations.

2. It should be valuable to study the effects of interactions between asphaltene model compound and other contributors to W/O emulsion stability, i.e. resins, waxes and solids on their interfacial behavior.

3. To further advance the field, it is important to study a mixture of several well-defined asphaltene model compounds to mimic real asphaltenes, understanding their interfacial properties and emulsification stability.

References

(1) Alberta Oil Sands Industry Quarterly Update, Winter 2015.

(2) Masliyah, J. H.; Xu, Z.; Czarnecki, J. A.; Dabros, M. *Handbook on Theory and Practice of Bitumen Recovery from Athabasca Oil Sands*. Cochrane, Alta.: Kingsley Knowledge Pub.: 2011.

(3) http://albertacanada.com/business/industries/og-conventional-crude-oil-and-oil-sands.aspx.

(4) http://www.energy.alberta.ca/About_Us/1133.asp.

(5) Masliyah, J.; Zhou, Z. J.; Xu, Z.; Czarnecki, J.; Hamza, H. Understanding Water‐Based Bitumen Extraction from Athabasca Oil Sands. *Can. J. Chem. Eng.* **2004,** *82*, 628-654.

(6) Natarajan, A.; Xie, J.; Wang, S.; Masliyah, J.; Zeng, H.; Xu, Z. Understanding Molecular Interactions of Asphaltenes in Organic Solvents Using a Surface Force Apparatus. *J. Phys. Chem. C* **2011,** *115*, 16043-16051.

(7) Long, Y.; Dabros, T.; Hamza, H. Stability and Settling Characteristics of Solvent-Diluted Bitumen Emulsions. *Fuel* **2002,** *81*, 1945-1952.

(8) Peramanu, S.; Pruden, B. B.; Rahimi, P. Molecular Weight and Specific Gravity Distributions for Athabasca and Cold Lake Bitumens and Their Saturate, Aromatic, Resin, and Asphaltene Fractions. *Ind. Eng. Chem. Res.* **1999,** *38*, 3121-3130.

(9) Yang, X.; Czarnecki, J. The Effect of Naphtha to Bitumen Ratio on Properties of Water in Diluted Bitumen Emulsions. *Colloids Surf., A* **2002,** *211*, 213-222.

(10) Rao, F.; Liu, Q. Froth Treatment in Athabasca Oil Sands Bitumen Recovery Process: A Review. *Energy Fuels* **2013,** *27*, 7199-7207.

(11) Long, Y.; Dabros, T.; Hamza, H. Selective Solvent Deasphalting for Heavy Oil Emulsion Treatment. In *Asphaltenes, Heavy Oils, and Petroleomics*, Springer: 2007; pp 511-547.

(12) Shelfantook, W. E. A Perspective on the Selection of Froth Treatment Processes. *Can. J. Chem. Eng.* **2004,** *82*, 704-709.

(13) Lissant, K. J. *Emulsions and Emulsion Technology*. Dekker: New York, 1974.

(14) Sjöblom, J. *Encyclopedic Handbook of Emulsion Technology.* Marcel Dekker: New York, 2001.

(15) Binks, B. P. *Modern Aspects of Emulsion Science. [Electronic Resource]*. Royal Society of Chemistry: Cambridge, 1998.

(16) Knudsen, A.; Nordgård, E. L.; Diou, O.; Sjöblom, J. Methods to Study Naphthenate Formation in W/O Emulsions by the Use of a Tetraacid Model Compound. *J. Dispersion Sci. Technol.* **2012,** *33*, 1514-1524.

(17) *Emulsion Science and Technology*; Tadros, T. F., Eds.; Wiley-VCH: 2009.

(18) Reed, S. G.; Bertholet, S.; Coler, R. N.; Friede, M. New Horizons in Adjuvants for Vaccine Development. *Trends Immunol.* **2009,** *30*, 23-32.

(19) Harbottle, D.; Liang, C.; El-Thaher, N.; Liu, Q.; Masliyah, J.; Xu, Z. Particle-Stabilized Emulsions in Heavy Oil Processing. In *Particle-Stabilized Emulsions and Colloids*, Ngai, T. and Bon, S. A. F., Eds.; Royal Society of Chemistry: 2014; pp 283-316.

(20) Little, R. C. Breaking Emulsions of Water in Navy Fuel Oils. *Fuel* **1974,** *53*, 246-252.

(21) Shetty, C. S.; Nikolov, A. D.; Wasan, D. T.; Bhattacharyya, B. R. Demulsification of Water in Oil Emulsions Using Water Soluble Demulsifiers. *J. Dispersion Sci. Technol.* **1992,** *13*, 121-133.

(22) Dodd, C. G. The Rheological Properties of Films at Crude Petroleum-Water Interfaces. *J. Phys. Chem.* **1960,** *64*, 544-550.

(23) Sjöblom, J.; Hemmingsen, P.; Kallevik, H. The Role of Asphaltenes in Stabilizing Water-in-Crude Oil Emulsions. In *Asphaltenes, Heavy Oils, and Petroleomics*, Mullins, O., Sheu, E., Hammami, A., and Marshall, A., Eds.; Springer: New York, 2007; pp 549-587.

(24) McLean, J. D.; Kilpatrick, P. K. Effects of Asphaltene Solvency on Stability of Water-in-Crude-Oil Emulsions. *J. Colloid Interface Sci.* **1997,** *189*, 242-253.

(25) McLean, J. D.; Kilpatrick, P. K. Effects of Asphaltene Aggregation in Model Heptane–Toluene Mixtures on Stability of Water-in-Oil Emulsions. *J. Colloid Interface Sci.* **1997,** *196*, 23-34.

(26) Taylor, S. E. Emulsions: Fundamentals and Applications in the Petroleum Industry. *Chem. Ind.* **1992,** *20*, 770-773.

(27) Johansen, E. J.; Skjärvö, I. M.; Lund, T.; Sjöblom, J.; Söderlund, H.; Boström, G. Water-in-Crude Oil Emulsions from the Norwegian Continental Shelf Part I. Formation, Characterization and Stability Correlations. *Colloids Surf.* **1988,** *34*, 353-370.

(28) Isaacs, E. E.; Huang, H.; Babchin, A. J.; Chow, R. S. Electroacoustic Method for Monitoring the Coalescence of Water-in-Oil Emulsions. *Colloids Surf.* **1990,** *46*, 177-192.

(29) Hassander, H.; Johansson, B.; Törnell, B. The Mechanism of Emulsion Stabilization by Small Silica (Ludox) Particles. *Colloids Surf.* **1989,** *40*, 93-105.

(30) Papirer, E.; Bourgeois, C.; Siffert, B.; Balard, H. Chemical Nature and Water/Oil Emulsifying Properties of Asphaltenes. *Fuel* **1982,** *61*, 732-734.

(31) Aveyard, R.; Binks, B. P.; Fletcher, P. D. I.; Lu, J. R. The Resolution of Water-in-Crude Oil Emulsions by the Addition of Low Molar Mass Demulsifiers. *J. Colloid Interface Sci.* **1990,** *139*, 128-138.

(32) Tambe, D. E.; Sharma, M. M. Factors Controlling the Stability of Colloid-Stabilized Emulsions: I. An Experimental Investigation. *J. Colloid Interface Sci.* **1993,** *157*, 244-253.

(33) Ali, M. F.; Alqam, M. H. The Role of Asphaltenes, Resins and Other Solids in the Stabilization of Water in Oil Emulsions and Its Effects on Oil Production in Saudi Oil Fields. *Fuel* **2000,** *79*, 1309-1316.

(34) Yan, N.; Gray, M. R.; Masliyah, J. H. On Water-in-Oil Emulsions Stabilized by Fine Solids. *Colloids Surf., A* **2001,** *193*, 97-107.

(35) Sullivan, A. P.; Kilpatrick, P. K. The Effects of Inorganic Solid Particles on Water and Crude Oil Emulsion Stability. *Ind. Eng. Chem. Res.* **2002,** *41*, 3389-3404.

(36) *Structures and Dynamics of Asphaltenes*; Mullins, O. C.; Sheu, E. Y., Eds.; Plenum Press: New York, 1998.

(37) Speight, J. G. *The Chemistry and Technology of Petroleum.* 4th Ed.; CRC Press: London, 2007.

(38) Buenrostro-Gonzalez, E.; Groenzin, H.; Lira-Galeana, C.; Mullins, O. C. The Overriding Chemical Principles That Define Asphaltenes. *Energy Fuels* **2001,** *15*, 972-978.

(39) Czarnecki, J.; Moran, K. On the Stabilization Mechanism of Water-in-Oil Emulsions in Petroleum Systems. *Energy Fuels* **2005,** *19*, 2074-2079.

(40) Spiecker, P. M.; Gawrys, K. L.; Kilpatrick, P. K. Aggregation and Solubility Behavior of Asphaltenes and Their Subfractions. *J. Colloid Interface Sci.* **2003,** *267*, 178-193.

(41) Wattana, P.; Fogler, H. S.; Yen, A.; Carmen Garcìa, M. D.; Carbognani, L. Characterization of Polarity-Based Asphaltene Subfractions. *Energy Fuels* **2005,** *19*, 101-110.

(42) Merdrignac, I.; Espinat, D. Physicochemical Characterization of Petroleum Fractions: The State of the Art. *Oil Gas Sci. Technol.* **2007,** *62*, 7-32.

(43) Akbarzadeh, K.; Hammami, A.; Kharrat, A.; Zhang, D.; Allenson, S.; Creek, J.; Kabir, S.; Jamaluddin, A.; Marshall, A. G.; Nalco Energy Services, L. P. Asphaltenes - Problematic but Rich in Potential. *Oilfield Rev.* **2007,** *19*, 22-43.

(44) Mullins, O. C.; Martínez-Haya, B.; Marshall, A. G. Contrasting Perspective on Asphaltene Molecular Weight. This Comment Vs the Overview of A. A. Herod, K. D. Bartle, and R. Kandiyoti. *Energy Fuels* **2008,** *22*, 1765-1773.

(45) Groenzin, H.; Mullins, O. C. Molecular Size and Structure of Asphaltenes from Various Sources. *Energy Fuels* **2000,** *14*, 677-684.

(46) Qian, K.; Edwards, K. E.; Siskin, M.; Olmstead, W. N.; Mennito, A. S.; Dechert, G. J.; Hoosain, N. E. Desorption and Ionization of Heavy Petroleum Molecules and Measurement of Molecular Weight Distributions. *Energy Fuels* **2007,** *21*, 1042-1047.

(47) Merdrignac, I.; Desmazieres, B.; Terrier, P.; Delobel, A.; Laprevote, O., Analysis of Raw and Hydrotreated Asphaltenes Using Off-Line and on-Line Sec/Ms Coupling. In *Proceedings of the Heavy Organic Deposition, Los Cabos, Baja California, Mexico*, 2004.

(48) Schneider, M. H.; Andrews, A. B.; Mitra-Kirtley, S.; Mullins, O. C. Asphaltene Molecular Size by Fluorescence Correlation Spectroscopy. *Energy Fuels* **2007,** *21*, 2875-2882.

(49) Freed, D. E.; Lisitza, N. V.; Sen, P. N.; Song, Y.-Q. Molecular Composition and Dynamics of Oils from Diffusion Measurements. In *Asphaltenes, Heavy Oils, and Petroleomics*, Springer: 2007; pp 279-299.

(50) Kuznicki, T.; Masliyah, J. H.; Bhattacharjee, S. Molecular Dynamics Study of Model Molecules Resembling Asphaltene-Like Structures in Aqueous Organic Solvent Systems. *Energy Fuels* **2008,** *22*, 2379-2389.

(51) Gawrys, K. L.; Matthew Spiecker, P.; Kilpatrick, P. K. The Role of Asphaltene Solubility and Chemical Composition on Asphaltene Aggregation. *Pet. Sci. Technol.* **2003,** *21*, 461-489.

(52) Sheremata, J. M.; Gray, M. R.; Dettman, H. D.; McCaffrey, W. C. Quantitative Molecular Representation and Sequential Optimization of Athabasca Asphaltenes. *Energy Fuels* **2004,** *18*, 1377-1384.

(53) Trbovich, M. G.; King, G. E. In *Asphaltene Deposit Removal: Long-Lasting Treatment with a Co-Solvent*, Society of Petroleum Engineers: 1991.

(54) Leontaritis, K. J.; Ali Mansoori, G. Asphaltene Deposition: A Survey of Field Experiences and Research Approaches. *J. Pet. Sci. Eng.* **1988,** *1*, 229-239.

(55) Khanifar, A.; Demiral, B.; Alian, S.; Darman, N. Study of Asphaltene Precipitation and Deposition Phenomenon. Presented at the National Postgraduate Conference, Kuala Lumpur, September 19-20, 2011.

(56) Hammami, A.; Phelps, C. H.; Monger-McClure, T.; Little, T. M. Asphaltene Precipitation from Live Oils: An Experimental Investigation of Onset Conditions and Reversibility. *Energy Fuels* **2000,** *14*, 14-18.

(57) Buenrostro-Gonzalez, E.; Lira-Galeana, C.; Gil-Villegas, A.; Wu, J. Asphaltene Precipitation in Crude Oils: Theory and Experiments. *AIChE J.* **2004,** *50*, 2552-2570.

(58) Almehaideb, R. A. Asphaltene Precipitation and Deposition in the near Wellbore Region: A Modeling Approach. *J. Pet. Sci. Eng.* **2004,** *42*, 157-170.

(59) Hirschberg, A.; DeJong, L. N. J.; Schipper, B. A.; Meijer, J. G. Influence of Temperature and Pressure on Asphaltene Flocculation. *Society of Petroleum Engineers Journal* **1984,** *24*, 283-293.

(60) James, N. E.; Mehrotra, A. K. V‑L‑S Multiphase Equilibrium in Bitumen‑Diluent Systems. *Can. J. Chem. Eng.* **1988,** *66*, 870-878.

(61) David Ting, P.; Hirasaki, G. J.; Chapman, W. G. Modeling of Asphaltene Phase Behavior with the Saft Equation of State. *Pet. Sci. Technol.* **2003,** *21*, 647-661.

(62) Correra, S., Donnaio, F., OCCAM, Onset-Constrained Colloidal Asphaltene Model. Presented at the SPE Int. Symp. on Formation Damage, Lafayette, LA, February 23-24, 2000; SPE 58724.

(63) Pan, H.; Firoozabadi, A. Thermodynamic Micellization Model for Asphaltene Precipitation from Reservoir Crudes at High Pressures and Temperatures. *SPE Prod. Facil.* **2000,** *15*, 58-65.

(64) Akbarzadeh, K.; Zhongxin, H. U. O.; Broze, G. Flow-through Tests Advance Researchers' Understanding of Asphaltene Deposition. *World oil* **2010,** *231*, 105-107.

(65) Dabros, T.; Yeung, A.; Masliyah, J.; Czarnecki, J. Emulsification through Area Contraction. *J. Colloid Interface Sci.* **1999,** *210*, 222-224.

(66) Spiecker, P. M.; Kilpatrick, P. K. Interfacial Rheology of Petroleum Asphaltenes at the Oil−Water Interface. *Langmuir* **2004,** *20*, 4022-4032.

(67) Harbottle, D.; Chen, Q.; Moorthy, K.; Wang, L.; Xu, S.; Liu, Q.; Sjöblom, J.; Xu, Z. Problematic Stabilizing Films in Petroleum Emulsions: Shear Rheological Response of Viscoelastic Asphaltene Films and the Effect on Drop Coalescence. *Langmuir* **2014,** *30*, 6730-6738.

(68) Gao, S.; Moran, K.; Xu, Z.; Masliyah, J. Role of Bitumen Components in Stabilizing Water-in-Diluted Oil Emulsions. *Energy Fuels* **2009,** *23*, 2606-2612.

(69) Moran, K.; Czarnecki, J. Competitive Adsorption of Sodium Naphthenates and Naturally Occurring Species at Water-in-Crude Oil Emulsion Droplet Surfaces. *Colloids Surf., A* **2007,** *292*, 87-98.

(70) Gao, S.; Moran, K.; Xu, Z.; Masliyah, J. Role of Naphthenic Acids in Stabilizing Water-in-Diluted Model Oil Emulsions. *J. Phys. Chem. B* **2010,** *114*, 7710-7718.

(71) Ese, M. H.; Yang, X.; Sjöblom, J. Film Forming Properties of Asphaltenes and Resins. A Comparative Langmuir–Blodgett Study of Crude Oils from North Sea, European Continent and Venezuela. *Colloid Polym. Sci.* **1998,** *276*, 800-809.

(72) Zhang, L. Y.; Xu, Z.; Masliyah, J. H. Characterization of Adsorbed Athabasca Asphaltene Films at Solvent-Water Interfaces Using a Langmuir Interfacial Trough. *Ind. Eng. Chem. Res.* **2005,** *44*, 1160-1174.

(73) Zhang, L. Y.; Lawrence, S.; Xu, Z.; Masliyah, J. H. Studies of Athabasca Asphaltene Langmuir Films at Air−Water Interface. *J. Colloid Interface Sci.* **2003,** *264*, 128-140.

(74) Zhang, L. Y.; Lopetinsky, R.; Xu, Z.; Masliyah, J. H. Asphaltene Monolayers at a Toluene/Water Interface. *Energy Fuels* **2005,** *19*, 1330-1336.

(75) Zhang, L. Y.; Breen, P.; Xu, Z.; Masliyah, J. H. Asphaltene Films at a Toluene/Water Interface. *Energy Fuels* **2007,** *21*, 274-285.

(76) Ese, M.-H.; Galet, L.; Clausse, D.; Sjöblom, J. Properties of Langmuir Surface and Interfacial Films Built up by Asphaltenes and Resins: Influence of Chemical Demulsifiers. *J. Colloid Interface Sci.* **1999,** *220*, 293-301.

(77) Zhang, L. Y.; Xu, Z.; Masliyah, J. H. Langmuir and Langmuir-Blodgett Films of Mixed Asphaltene and a Demulsifier. *Langmuir* **2003,** *19*, 9730-9741.

(78) Yarranton, H. W.; Sztukowski, D. M.; Urrutia, P. Effect of Interfacial Rheology on Model Emulsion Coalescence: I. Interfacial Rheology. *J. Colloid Interface Sci.* **2007,** *310*, 246-252.

(79) Alvarez, G.; Poteau, S.; Argillier, J.-F. o.; Langevin, D.; Salager, J.-L. Heavy Oil−Water Interfacial Properties and Emulsion Stability: Influence of Dilution. *Energy Fuels* **2009,** *23*, 294-299.

(80) Sztukowski, D. M.; Yarranton, H. W. Rheology of Asphaltene-Toluene/Water Interfaces. *Langmuir* **2005,** *21*, 11651-11658.

(81) Freer, E. M.; Radke, C. J. Relaxation of Asphaltenes at the Toluene/Water Interface: Diffusion Exchange and Surface Rearrangement. *J. Adhes.* **2004,** *80*, 481-496.

(82) Acevedo, S.; Escobar, G.; Gutiérrez, L. B.; Rivas, H.; Gutiérrez, X. Interfacial Rheological Studies of Extra-Heavy Crude Oils and Asphaltenes: Role of the Dispersion Effect of Resins in the Adsorption of Asphaltenes at the Interface of Water-in-Crude Oil Emulsions. *Colloids Surf., A* **1993,** *71*, 65-71.

(83) Fan, Y.; Simon, S.; Sjöblom, J. Interfacial Shear Rheology of Asphaltenes at Oil–Water Interface and Its Relation to Emulsion Stability: Influence of Concentration, Solvent Aromaticity and Nonionic Surfactant. *Colloids Surf., A* **2010,** *366*, 120-128.

(84) Verruto, V. J.; Le, R. K.; Kilpatrick, P. K. Adsorption and Molecular Rearrangement of Amphoteric Species at Oil−Water Interfaces. *J. Phys. Chem. B* **2009,** *113*, 13788-13799.

(85) Sjöblom, J.; Simon, S.; Xu, Z. Model Molecules Mimicking Asphaltenes. *Adv. Colloid Interface Sci.* **2015,** *218*, 1-16.

(86) Akbarzadeh, K.; Bressler, D. C.; Wang, J.; Gawrys, K. L.; Gray, M. R.; Kilpatrick, P. K.; Yarranton, H. W. Association Behavior of Pyrene Compounds as Models for Asphaltenes. *Energy Fuels* **2005,** *19*, 1268-1271.

(87) Rakotondradany, F.; Fenniri, H.; Rahimi, P.; Gawrys, K. L.; Kilpatrick, P. K.; Gray, M. R. Hexabenzocoronene Model Compounds for Asphaltene Fractions: Synthesis & Characterization. *Energy Fuels* **2006,** *20*, 2439-2447.

(88) Tan, X.; Fenniri, H.; Gray, M. R. Pyrene Derivatives of 2, 2′ -Bipyridine as Models for Asphaltenes: Synthesis, Characterization, and Supramolecular Organization. *Energy Fuels* **2007,** *22*, 715-720.

(89) Kuznicki, T.; Masliyah, J. H.; Bhattacharjee, S. Aggregation and Partitioning of Model Asphaltenes at Toluene−Water Interfaces: Molecular Dynamics Simulations. *Energy Fuels* **2009,** *23*, 5027-5035.

(90) Jian, C.; Tang, T.; Bhattacharjee, S. Probing the Effect of Side-Chain Length on the Aggregation of a Model Asphaltene Using Molecular Dynamics Simulations. *Energy Fuels* **2013,** *27*, 2057-2067.

(91) Nordgård, E. L.; Landsem, E.; Sjöblom, J. Langmuir Films of Asphaltene Model Compounds and Their Fluorescent Properties. *Langmuir* **2008,** *24*, 8742-8751.

(92) Nordgård, E. L. k.; Sjöblom, J. Model Compounds for Asphaltenes and C80 Isoprenoid Tetraacids. Part I: Synthesis and Interfacial Activities. *J. Dispersion Sci. Technol.* **2008,** *29*, 1114-1122.

(93) Wang, J.; van der Tuuk Opedal, N.; Lu, Q.; Xu, Z.; Zeng, H.; Sjöblom, J. Probing Molecular Interactions of an Asphaltene Model Compound in Organic Solvents Using a Surface Forces Apparatus (SFA). *Energy Fuels* **2012,** *26*, 2591-2599.

(94) Wang, J.; Lu, Q.; Harbottle, D.; Sjöblom, J.; Xu, Z.; Zeng, H. Molecular Interactions of a Polyaromatic Surfactant C5pe in Aqueous Solutions Studied by a Surface Forces Apparatus. *J. Phys. Chem. B* **2012,** *116*, 11187-11196.

(95) Teklebrhan, R. B.; Ge, L.; Bhattacharjee, S.; Xu, Z.; Sjöblom, J. Initial Partition and Aggregation of Uncharged Polyaromatic Molecules at the Oil-Water Interface: A Molecular Dynamics Simulation Study. *J. Phys. Chem. B* **2014,** *118*, 1040-1051.

(96) Nordgård, E. L.; Sørland, G.; Sjöblom, J. Behavior of Asphaltene Model Compounds at W/O Interfaces. *Langmuir* **2010,** *26*, 2352-2360.

(97) Grimes, B. A.; Dorao, C. A.; Simon, S.; Nordgard, E. L.; Sjöblom, J. Analysis of Dynamic Surfactant Mass Transfer and Its Relationship to the Transient Stabilization of Coalescing Liquid-Liquid Dispersions. *J. Colloid Interface Sci.* **2010,** *348*, 479-490.

(98) Nenningsland, A. L.; Gao, B.; Simon, S.; Sjöblom, J. Comparative Study of Stabilizing Agents for Water-in-Oil Emulsions. *Energy Fuels* **2011,** *25*, 5746-5754.

(99) Alshareef, A. H.; Scherer, A.; Tan, X.; Azyat, K.; Stryker, J. M.; Tykwinski, R. R.; Gray, M. R. Effect of Chemical Structure on the Cracking and Coking of Archipelago Model Compounds Representative of Asphaltenes. *Energy Fuels* **2012,** *26*, 1828-1843.

(100) Alshareef, A. H.; Scherer, A.; Stryker, J. M.; Tykwinski, R. R.; Gray, M. R. Thermal Cracking of Substituted Cholestane–Benzoquinoline Asphaltene Model Compounds. *Energy Fuels* **2012,** *26*, 3592-3603.

(101) Arashiro, E. Y.; Demarquette, N. R. Use of the Pendant Drop Method to Measure Interfacial Tension between Molten Polymers. *Mater. Res.* **1999,** *2*, 23-32.

(102) Vandebril, S.; Franck, A.; Fuller, G. G.; Moldenaers, P.; Vermant, J. A Double Wall-Ring Geometry for Interfacial Shear Rheometry. *Rheol. Acta* **2009,** *49*, 131-144.

(103) Solovyev, A.; Zhang, L. Y.; Xu, Z.; Masliyah, J. H. Langmuir Films of Bitumen at Oil/Water Interfaces. *Energy Fuels* **2006,** *20*, 1572-1578.

(104) Xu, R.; Dickinson, E.; Murray, B. S. Morphological Changes in Adsorbed Protein Films at the Oil-Water Interface Subjected to Compression, Expansion, and Heat Processing. *Langmuir* **2008,** *24*, 1979-1988.

(105) Murray, B. S.; Xu, R.; Dickinson, E. Brewster Angle Microscopy of Adsorbed Protein Films at Air–Water and Oil–Water Interfaces after Compression, Expansion and Heat Processing. *Food Hydrocolloids* **2009,** *23*, 1190-1197.

(106) Cadena-Nava, R. D.; Cosultchi, A.; Ruiz-Garcia, J. Asphaltene Behavior at Interfaces. *Energy Fuels* **2007,** *21*, 2129-2137.

(107) Schirmeisen, André; Anczykowski, B.; Fuchs, H. Dynamic Modes of Atomic Force Microscopy. in *Handbook of Nanotechnology*, 2nd edition; Bhushan, B., Eds.; Springer: Berlin, 2007; pp 737-765.

(108) http://www.biolinscientific.com/technology/l-lb-ls-technique/.

(109) http://www.charfac.umn.edu/instruments/5500_Users_Guide.pdf.

(110) Wang, L.; Dang-Vu, T.; Xu, Z.; Masliyah, J. H. Use of Short-Chain Amine in Processing of Weathered/Oxidized Oil Sands Ores. *Energy Fuels* **2010,** *24*, 3581-3588.

(111) Bendure, R. L. Dynamic Surface Tension Determination with the Maximum Bubble Pressure Method. *J. Colloid Interface Sci.* **1971,** *35*, 238-248.

(112) Bouriat, P.; El Kerri, N.; Graciaa, A.; Lachaise, J. Properties of a Two-Dimensional Asphaltene Network at the Water-Cyclohexane Interface Deduced from Dynamic Tensiometry. *Langmuir* **2004,** *20*, 7459-7464.

(113) Sollich, P.; Lequeux, F.; Hébraud, P.; Cates, M. E. Rheology of Soft Glassy Materials. *Phys. Rev. Lett.* **1997,** *78*, 2020-2023.

(114) Srivastava, S.; Leiske, D.; Basu, J. K.; Fuller, G. G. Interfacial Shear Rheology of Highly Confined Glassy Polymers. *Soft Matter* **2011,** *7*, 1994-2000.

(115) Allen, R.; Bao, Z.; Fuller, G. G. Oriented, Polymer-Stabilized Carbon Nanotube Films: Influence of Dispersion Rheology. *Nanotechnology* **2013,** *24*, 015709.

(116) Seoane, R.; Minones, J.; Conde, O.; Minones, J.; Casas, M.; Iribarnegaray, E. Thermodynamic and Brewster Angle Microscopy Studies of Fatty Acid/Cholesterol Mixtures at the Air/Water Interface. *J. Phys. Chem. B* **2000,** *104*, 7735-7744.

(117) Gopal, A.; Lee, K. Y. C. Morphology and Collapse Transitions in Binary Phospholipid Monolayers. *J. Phys. Chem. B* **2001,** *105*, 10348-10354.

(118) Birdi, K. S.; Vu, D. T. Structures of Collapsed Lipid Monolayers Investigated as Langmuir-Blodgett Films by Atomic Force Microscopy. *Langmuir* **1994,** *10*, 623-625.

(119) Fainerman, V. B.; Kovalchuk, V. I.; Lucassen-Reynders, E. H.; Grigoriev, D. O.; Ferri, J. K.; Leser, M. E.; Michel, M.; Miller, R.; Möhwald, H. Surface-Pressure Isotherms of Monolayers Formed by Microsize and Nanosize Particles. *Langmuir* **2006,** *22*, 1701-1705.

(120) Harkins, W. D.; Boyd, E. The States of Monolayers. *J. Phys. Chem.* **1941,** *45*, 20-43.

(121) Antunes, P. A.; Constantino, C. J. L.; Aroca, R. F.; Duff, J. Langmuir and Langmuir-Blodgett Films of Perylene Tetracarboxylic Derivatives with Varying Alkyl Chain Length: Film Packing and Surface-Enhanced Fluorescence Studies. *Langmuir* **2001,** *17*, 2958-2964.

(122) Varadaraj, R.; Brons, C. Molecular Origins of Crude Oil Interfacial Activity. Part 4: Oil–Water Interface Elasticity and Crude Oil Asphaltene Films. *Energy Fuels* **2012,** *26*, 7164-7169.

Appendix A   Procedure of Γ_{max} and A_i calculation

(1) Calculate the density of C5Pe in xylene solution.

$$\rho_{solution} = \frac{\rho_{xylene} \times 1m^3 + MW_{C5Pe} \times c_{C5Pe} \times 1m^3}{1m^3} \qquad (A.1)$$

Where $\rho_{xylene} = 865$ kg/m^3, $MW_{C5Pe} = 689$ g/mol, and c_{C5Pe} is the concentration of C5Pe.

(2) Convert the unit of the concentration of C5Pe solution from mM to mol/kg (mM = mol/m^3).

$$c_{mol/kg} = \frac{c_{mM}}{\rho_{solution}} \qquad (A.2)$$

Table A.1 Concentration conversion of C5Pe in xylene solutions.

concentration, mM	density, kg/m^3	concentration, mol/kg
1×10^{-4}	8.65×10^2	1.16×10^{-7}
5×10^{-4}	8.65×10^2	5.78×10^{-7}
1×10^{-3}	8.66×10^2	1.16×10^{-6}
3×10^{-3}	8.67×10^2	3.46×10^{-6}
5×10^{-3}	8.68×10^2	5.76×10^{-6}
0.01	8.72×10^2	1.15×10^{-5}
0.03	8.86×10^2	3.39×10^{-5}
0.06	9.06×10^2	6.62×10^{-5}
0.1	9.34×10^2	1.07×10^{-4}
0.2	1.00×10^3	1.99×10^{-4}
0.3	1.07×10^3	2.80×10^{-4}
0.5	1.21×10^3	4.13×10^{-4}

(3) Calculate the slopes in the linear regions of interfacial tension isotherm.

Data points used for linear fit (c: concentration; γ: interfacial tension):

pH 4: c_1=0.003mM, γ_1= 26.97mN/m; c_2=0.01mM, γ_2= 23.61mN/m; c_3=0.06mM, γ_3= 17.85mN/m.

pH 7: c_1=0.01mM, γ_2= 22.54mN/m; c_2=0.03mM, γ_2= 15.27mN/m; c_3=0.06mM, γ_3= 9.74mN/m.

pH 9: c_1=0.01mM, γ_1= 14.52mN/m; c_2=0.03mM, γ_2= 5.76mN/m; c_3=0.06mM, γ_3= 0mN/m.

Table A.2 Derivative of interfacial tension with respect to natural log concentration of C5Pe solutions as a function of pH.

pH	4	7	9
Slope (dγ/dlnc)	-3.10×10^{-3}	-7.25×10^{-3}	-8.26×10^{-3}

(4) Calculate Γ_{max} using Gibbs equation based on the slopes gained in step 3. Gibbs equation:

$$\frac{-d\gamma}{RT} = \sum(\Gamma_i dlna_i) \tag{A.3}$$

Assumptions: ① the adsorption of major component (solvent) A is regarded as zero; ② solution is dilute, activity a can be replaced by concentration c.

For a two-component system, solvent A and solute B:

$$\frac{-d\gamma}{RT} = n\Gamma_B dlnc_B \tag{A.4}$$

Therefore,
$$\Gamma_B = -\frac{1}{nRT}\frac{d\gamma}{dlnc_B} \tag{A.5}$$

n=1 for solute without ionization; n=2 if solute is ionized.

(5) Calculate the area per molecule A_i.

$$A_i = \frac{1}{\Gamma_{max}N_A} \tag{A.6}$$